Coupled Consolidation Model for Negative Skin Friction on Piles in Clay Layers

A

Thesis

in

The Department of Building, Civil and Environmental Engineering

Presented in Partial Fulfillment of the Requirements

For the Degree of Master of Applied Science at

Concordia University

Montreal, Quebec, CANADA

January 2006

Your file Votre référence
ISBN: 0-494-14247-2
Our file Notre référence
ISBN: 0-494-14247-2

ABSTRACT

Coupled Consolidation Model for Negative Skin Friction on Piles in Clay Layers

Mohammad Azizul Hoque

Piles driven in clay are often subjected to indirect loading as a result of the surcharge applied on the surrounding area. During the drained period, both the pile and the soil undergo downward movements caused by the axial and the surcharge loading, respectively. Depending on the relative movement of the pile/soil system, positive and negative skin friction develop on the pile's shaft. Negative skin friction is the drag force that may be large enough to reduce the pile capacity and/or to overstress the pile's material causing fractures or perhaps structural failure or possibly pulling out the pile from the cap.

A numerical model was developed to simulate the case of a single pile driven in soft clay layer overlying a deep deposit. Coupled consolidation method of analysis is adopted to predict time/settlement/skin friction distribution relationships. The model is an axisymmetric that uses the finite element technique combined with the soil responses according to Mohr-Coulomb criteria. The model was first tested against the results predicted by the classic theories for bearing capacity of pile foundations on clay. Furthermore, the model was validated with the results of three full scale field tests available in the literature.

Upon achieving satisfactory results, the numerical model was then used to generate data for a wide ranges of the parameters believed to govern the case of single pile driven in clay layers and subjected to surcharge loading. Time dependent-skin friction, axial loads, and fluctuation of neutral plane location are analyzed under different pile/loading/clay conditions. A sensitivity analysis is then performed to examine the effect of the thickness ratio of the clay layers, cohesion ratio, and the surcharge loads that govern the distribution of skin friction, neutral plane location, and the bearing capacity of the pile.

Based on the results of the present investigation, design theory and procedures are presented to predict the location of the neutral plane and to estimate the drag force acting on the pile's shaft for a given pile/soil/loading condition. In case of excessive drag force, coating the pile's shaft should be coated with a thin layer of bitumen to eliminate or minimize to the drag force. Design charts are presented herein for practicing use and further to provide a mean for the designers to establish the need and the extent of the pile coating.

ACkNOWLEDGEMENTS

I would like to express my sincere gratitude to my supervisor, Professor **Adel M. Hanna,** for his valuable guidance, constant support and encouragement throughout the course of this work, which made it possible to complete this research. I am honored to carry out the present investigation under his supervision.

I would like to thank Dr. Mohab Sabry for his assistance particularly in developing the numerical model and the encouragement during carry out this work.

Table of Contents

List of Figures

List of Tables

CHAPTER 1

INTRODUCTION

1.1 Preface

The necessity of pile foundations is owing to the rapid growth of civilization. Pile foundations are often used in case of heavy loads and or to minimize the foundation settlements. Piles driven into clay are often subjected to indirect loading as a result of the surcharge applied on the surrounding area. During the drained period, both the piles and the soil undergo downward movements caused by the axial and the surcharge loading, respectively. Soils adjacent to pile surface will experience settlement due to the movement of the freshly placed fill material, pile driving, and lowering of ground water table. The negative skin friction along the pile's shaft develops when the settlement of the surrounding soil is larger than the settlement of the pile. Depending on the relative movement of the pile/soil system, positive and negative skin friction develop on the pile's shaft. Negative skin friction is the drag force that may be large enough to reduce the pile capacity and/or to overstress the pile's material causing fractures or perhaps structural failure of the pile, and/or possibly pulling out the pile from the cap.

The downdrag force induced on the pile is a loading condition, which often ignored or overlooked. When negative skin friction is expected, it is important to determine an appropriate amount and extend of the downdrag force on the pile's shaft. In order to

achieve this goal, the location of neutral plane, which separate the positive from the negative skin frictions on the pile shaft has to be determined. Furthermore, considering that the settlement of surrounding soil is a time dependent process, the location of neutral plane may fluctuate with time and accordingly the drag force. However, the location of the neutral plane, which produces the maximum drag force, should be considered for design. Down drag loads are often reduced or minimized using bitumen coating on the shaft area above the neutral plane or by jacketing the pile surface.

1.2 Thesis outline

Chapter 2 presents the literature review on the negative skin friction, evaluation of the drag force and method of analyses available. Chapter 3 describes the numerical model developed to simulate the problem stated and model validation. Chapter 4 presents the results of the present numerical model, sensitivity analyses, and the development of design charts and design procedure. Chapter 5 presents the conclusions and recommendations for future work.

1.3 Objective of the Thesis

To develop a numerical model that simulates the case of pile driven in a soft clay layer overlying deep deposit. The model will incorporate the coupled consolidation analysis to account for the time dependency. After validating the model, sensitivity analyses will be conducted on the parameters believed to govern this behavior. Design theory and procedure will be presented for practicing use.

CHAPTER 2

LITERATURE REVIEW

2.1 General

The recent development in determining the downdrag force one piles due to surcharge loading is reviewed in this chapter. It includes numerical analyses, laboratory and field testing. In general, the majority of the numerical models are based on the assumption that the soil will behave elastically (Lee 1993, Wong and Teh, 1995, and Poorooshab et al, 1996), while others developed theories for determining the location of the neutral plane as well as for the magnitude of downdrag (Matyas and Santamarina, 1994 and Hanna and Sharif, 2006). Few full-scale studies were carried out in order to investigate negative skin friction development (Bjerrum et al 1969, Endo et al 1969, Indraratna et al 1992). Nevertheless, no attempts were made to investigate the case of piles driven in a limited thickness of soft clay overlying deep deposit.

2.2 Review of Previous Work

Terzaghi and Peck (1948) suggested a conservative method for determining the down drag force on pile driven in soft clay. They assumed full mobilization of shear strength along the pile-soil interface up to pile toe for a single pile, or along the perimeter of pile group. Therefore, the neutral point (point of zero shear stress, or where the relative

movement between pile and soil is zero) is assumed to be located at the bearing stratum of the pile.

Buisson et al (1960) proposed that shear stress along the pile's shaft is related to the shear strain. Furthermore, they suggested that the relative movement between the pile and soil at some point along the pile length would be zero.

Poorooshasb and Bozozuk (1967) presented a closed form solution to an incompressible pile driven in soft clay and rest on bedrock. Surcharge load was applied on the surface of the clay layer and the case of double drainage was permitted. It was assumed that the pore water dissipation was not affected by the presence of the pile. The solution was carried out based on an upper bound plastic analysis. A kinematical admissible displacement field was adopted for this analysis that satisfies the overall equilibrium of the system. An elasto-plastic material model was considered that indicates an increase of stiffness of soil with depth.

Endo et al (1969) conducted insitu study on the negative skin friction using four instrumented steel piles during a period of three years in Japan. The piles were 43 m long, 600 mm diameter and driven at a spacing of 10m in order to avoid interferences between adjacent piles. The soil profile comprises of 10 m thick layer of silty sand overlying 25 m of silt below which an alternating layers of silt and sandy silt laid up to a depth of 44 m. They reported that a considerable settlement was experienced during the pile driven process. After three year period, the settlement of the ground surface was found to be 129 mm, most of which occurred below the depth of 20 m. The neutral plane was found at a

depth of 30 m below the ground surface, where the pile and the soil settlements were found to be 40 mm.

They pointed out that the axial force due to the negative skin friction is transmitted to the pile toe while it is being diminished by the positive skin friction acting on the pile below the neutral plane. Furthermore, they reported the ratio of the depth of the neutral plane to the length of the pile in compressible strata fell within a range of 0.73 to 0.78, irrespective of the variation in the manner in which pile toe was supported. The authors indicated that the negative skin friction required a span of time before it is fully developed. Furthermore, the negative skin friction showed no tendency to decrease with the decrease of the relative displacement velocity; moreover, the distribution of the axial force on piles was approximately symmetrical about the neutral plane.

Bjerrum et al (1969) carried out a major field testing program for the measurement of negative skin friction on steel pipe piles in Norway. The 500 mm diameter piles were driven to rock at 40 m depth. The soil profile was 13 m fill, placed over 27 m of soft clay overlying the bedrock. The water table was located at 2 m below the ground surface and small excess pore pressure was recorded during pile driving. After two years from the pile installation, the pile head was settled about 13.7 mm and the surrounding soil was settled about 70 mm. A very large down drag loads were developed on the pile's shaft that caused the yielding of the lower part. Negative skin friction was developed very quickly and only a little relative movement was required to generate the maximum down drag loads.

Poulos and Davis (1972) studied the change of the downdrag loads with time in an impermeable pile. A fully saturated soil was assumed to be consolidated due to surcharge loads. In this study, the probability of local yield between pile-soil interface and limited crushing of the pile due to excess loading was taken into consideration.

The study was carried out for one-dimensional consolidation settlement of the soil. The consolidation settlement was represented by the following equation.

$$S_i = \sum m_v . F_k (u_0 - u_t) L / n \quad \ldots\ldots\ldots\ldots\ldots\ldots\ldots\ldots\ldots\ldots\ldots\ldots\ldots\ldots (2.1)$$

Where m_v is the coefficient of volume change, u_0 and u_t are the excess pore pressure during installation and at time t later at a point k in the soil.

$F_k = 1$ for $k > i$ and 0.5 for $k = i$;

The solution for the maximum downdrag load in a pile was given by the following equation.

$$F_n^m = I_N \, S \, L^2 \quad \ldots\ldots\ldots\ldots\ldots\ldots\ldots\ldots\ldots\ldots\ldots\ldots\ldots\ldots\ldots\ldots\ldots\ldots (2.2)$$

Where I_N is the influence factor, S is the surcharge loading and L is the length of the pile. The final downdrag force can be attained by the following procedure. The maximum downdrag forces, F_n^m is multiplied by a correction factor if full slip does not occur, if installation delayed where consolidation has been permitted, or soil's Poisson ratio greater than zero.

Fellenius (1972) conducted experimental investigation on two instrumented precast concrete piles driven through 40m of soft clay and 15m into underlying silt and sand. The program was carried out in two consecutive phases: The first phase was to study the influence of the driving process of the pile and the consolidation of the clay for 465 days

started immediately after driving and up to the stage of pile loading .The second phase was to study the influence of applied load on the pile head for 800 days starting from the application of load until the end of the measurements.

It was observed that immediately after the pile installation, the forces in the pile increased rapidly and the rate of loading was linear after 5 to 7 months. A total of 550 kN load due to the down drag force was experienced after 495 days, 300 kN of which corresponded only to the consolidation of soil due to pile driving and the rest was due to regional settlement. It was found that the negative skin friction is 30 percent of the undrained shear strength, or 10 percent of the effective overburden pressure. After a consolidation period of 495 days the pile was loaded with 440 kN and an additional 360 kN was applied a year later.

Fellenius presented a design approach that takes negative skin friction into consideration in determining the allowable load on a single pile. The main feature of his approach was that the permanent and the transient working loads should be treated in connection with the negative skin friction. The ultimate bearing capacity Q_u of the pile is estimated based on the tip resistance Q_{utip} and a positive shaft resistance Fs in the non-settling soil layer as shown in Fig 2.1. However, no contribution of the negative shaft resistance in the upper soft layer is included in ultimate bearing capacity .After determining the ultimate bearing capacity of Q_u of the pile, the maximum drag load, F_{nmax} can be estimated from the strength properties of the settling soil without applying the usual reduction of the shear strength. If a transient load P_t on the pile head is smaller than twice the drag load F_{nmax}, the transient load will not be applied to the load in the lower portion of the pile. Thus the following equation applies:

$$P_p < Q_{utip} + Fs - Fn \quad \ldots\ldots\ldots\ldots\ldots\ldots\ldots\ldots\ldots\ldots\ldots\ldots (2.3)$$

Where, P_p is the permanent load on pile head.

Fellenius recommended partial factors of safety to be applied, thus above equation becomes

$$f_p . P_p < (1/f_q). (Q_{utip} + Fs) - f_n. F_n \quad \ldots\ldots\ldots\ldots\ldots\ldots\ldots(2.4)$$

Where,

fp, fq and fn are the factor of safety on the permanent load P_p, ultimate bearing capacity

Q_u and drag load F_n respectively.

If $2F_{nmax} < P_t$, the positive skin friction will be developed along the length of the pile and the equation (2.4) will then

$$f_t . P_t + (f_p . P_p) < (1/f_q). Q_u \quad \ldots\ldots\ldots\ldots\ldots\ldots\ldots\ldots\ldots(2.5)$$

Where f_t is the factor of safety on the transient load, P_t.

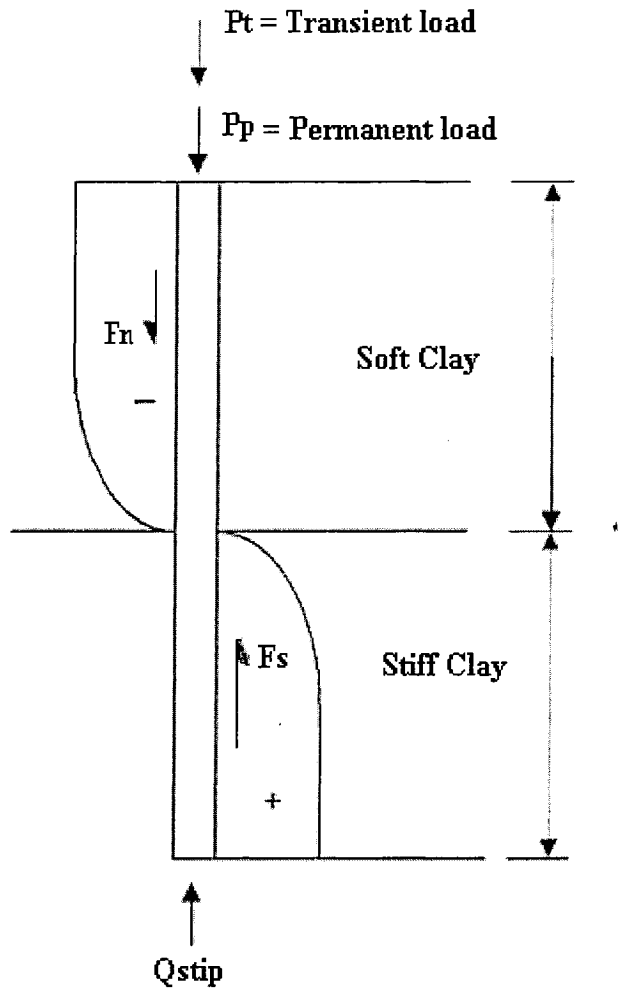

Fig. 2.1 Skin friction on a single pile installed in a soft soil layer overlying a non-settling soil (After Fellenius, 1972)

Bozuzuk (1972) measured the downdrag load on a 160 ft (49m) steel pipe pile floating in marine clay. He showed that the skin friction is the product of a combination effect of the insitu horizontal effective stresses, horizontal stresses due to the embankment loads, and the horizontal stresses due to differential settlement of the fill as shown in Fig. 2.2.

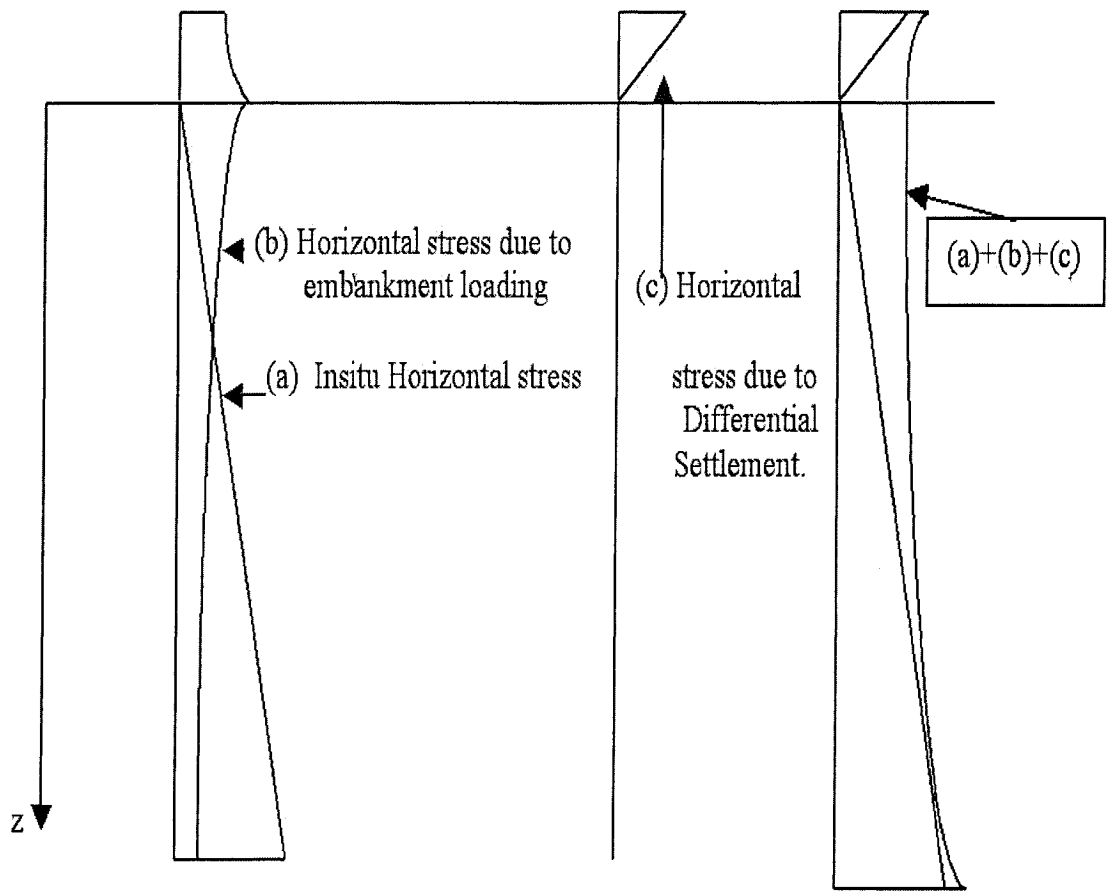

Fig. 2.2 Horizontal stresses acting on compressible clay layer (After Bozuzuk, 1972)

Considering a non-displacement type of circular pile driven at a depth L into a uniform isotropic clay deposit and the water table is located at the ground surface, the downdrag load due to the insitu horizontal effective stress can be given as:

$$F_n = \int_0^{L_{np}} M\, K_0 \gamma_s'(\tan\phi')ZCdz \quad \ldots\ldots\ldots\ldots\ldots\ldots\ldots\ldots\ldots\ldots (2.6)$$

where,

M : friction factor for the soil acting on the pile surface (0<M<1).

K_0 : coefficient relating horizontal to vertical effective stress.

γ_s' : submerged unit weight of soil.

ϕ' : effective friction angle of soil.

C : circumference of the pile.

The above equation can be simplified as:

$$F_n = \beta_1 C \int_0^{L_{np}} Z dz \quad \text{..... (2.7)}$$

Where, $\beta_1 = M\, K_0\, \gamma'_{s(}.\tan \phi')$

After the integration,

$$F_n = \beta_1 C \frac{L^2_{np}}{2} \quad \text{.....(2.8)}$$

This load will be resisted by the positive skin friction, F_p which will be developed on the pile from the neutral plane depth, L_{np} to the pile's tip.

$$F_p = \beta_2 C \frac{L^2 - L^2_{np}}{2} \quad \text{..... (2.9)}$$

In case of frictional piles (no end bearing load),

$$F_p = F_n$$

If $\beta_1 = \beta_2$

Then, Lnp = $L/\sqrt{2}$ which is the location of the neutral plane. The negative skin friction caused by the horizontal stresses developed due to construction of embankment is

$$F_n = M\,(\tan\phi')C \sum_{i=1}^{n_{L_{NP}}} \Delta L_i . \Delta\sigma_{x_i} \quad \text{..... (2.10)}$$

Furthermore, the positive skin friction is given as:

$$F_p = M\,(\tan\phi')C \sum_{i=n_{L_{NP}}}^{n_{L+1}} \Delta L_i \Delta\sigma_{x_i} \quad \ldots\ldots\ldots\ldots\ldots\ldots\ldots\ldots\ldots\ldots(2.11)$$

Where ΔL is the increment of length of pile under consideration and $\Delta\sigma_x$ is the average effective stress due to the embankment load acting on ΔL. Bozuzuk (1972) made a comparison of skin friction with soil strength and he concluded that there is little or no relation between the skin frictions applied on the pile surface and the in-situ shear strength of the soil. The upper part of the soil profile, where the relative movements between pile and soil are small and all excess pore pressures had dissipated; the unit skin friction approached but didn't exceed the drained strength. At the bottom of the pile, where the excess pore pressure and the relative movements between pile and soil are relatively large, the unit skin friction was decreased but didn't fall below the remoulded shear strength of the surrounding soil.

Walker and Darvall (1973) had performed field tests to investigate the magnitude and distribution of negative skin friction on piles and the efficiency of bitumen coatings in reducing drag loads due to negative skin friction. The tests involved the instrumentation and driving of two 760 mm diameter and 11 mm thick steel shell piles one of which was coated with bitumen to an average thickness of 1.5 mm.

This study was directed to evaluate the soil-structure interaction, which occurred during the development of the downdrag force on coated and uncoated piles. They concluded that large downdrag loads can be generated in uncoated piles due to small ground settlements. Negative skin friction appeared to be a function of ground settlements rather than effective stress. Bitumen coating is effective in reducing downdrag loads.

Tomlinson (1975) proposed a design method for calculating the magnitude of the downdrag forces of single piles. Field tests were conducted on piles driven into a relatively incompressible layer or into a compressible layer. In the first case, it was assumed that substantial amount of settlement leads to the mobilization of maximum negative skin. The relative movements between the pile and the soil in case of soft clay were about 1 % of the pile diameter to initiate maximum negative skin friction. He reported that when the pile was driven into a compressible layer, only the upper part of the pile up to the neutral plane will experience the negative skin friction.

Vesic (1977) reported that the negative skin friction could only be developed along the pile shaft when settlements of adjacent soil exceed 15 mm. He assumed that the magnitude of the downdrag loads is proportional to the effective vertical stress. Depending on the angle of shearing resistance, he proposed that the skin resistance factor (β) for uncoated piles in compressible clay and silt is fallen into the range of 0.15 to 0.30.

Fellenius (1988) proposed a unified design approach for piles and pile groups wherein capacity, residual compression, negative skin friction, and settlement of both the pile and the soil were considered. He suggested that the problem in designing for negative skin friction is one of the settlement issues, not of the bearing capacity problem. Four aspects were taken under consideration in order to carry out the design: the neutral plane location, structural capacity, settlement and the bearing capacity.

Increasing pile length can reduce the negative skin friction caused by excessive settlement, or decreasing pile diameter. When this type of measures are not practical, or economical, application of bitumen coating or other viscous coating to the pile surface will help in reducing the negative skin friction.

Leung et al (1991) reported a field test on the behavior of precast reinforced concrete piles driven through soft marine clay and founded in residual soil and weathered rock of sedimentary origin. Two instrumented piles were installed at two different locations in the Singapore port area in order to study the load transfer behavior of driven piles.

The variation of excess pore water pressures in the marine clay during pile installation was recorded and it was found that a rapid build up excess of pore pressure when the first segment of the pile was installed. Negative skin friction was developed due to the primary consolidation of the fill material, although it was in the site for about 10 years, and due to the clay consolidation for the excess pore pressure caused by the driving of the pile. Finally, the additional loading of the concrete deck and containers imposed on the fill when the piles were in service may have caused additional settlement. A little magnitude of negative skin friction was noted for the fill and the upper marine clay since these layers are relatively weak. Negative skin friction was developed in the lower marine clay about 10 kPa approximately 100 days after the deck was completed and it was increased to 22 kPa after 500 days.

The rate of the increase in the negative skin friction appeared to decreases with time. The rate of the dissipation of excess pore pressure is quicker for the upper marine

clay because of shorter drainage path and the slower for lower marine clay for longer drainage path.

Indraratna et al (1992) reported a field study on the downdarg loads acting on driven piles in soft Bangkok clay. They showed the results of short-term pullout tests and long-term full-scale measurements of negative skin friction. Their prediction was that the negative skin friction on driven piles in the long-term might be obtained using parameters of short-term pullout tests. Furthermore, they suggested that α and β parameters obtained from the short-term pullout tests agreed closely with the long-term measurements for total and effective stress methods. When the value of β is in between 0.1 and 0.2, the effective stress approach for calculating the negative skin friction is very effective.

In additional, they investigated the development of negative skin friction using finite element method. Since the development of the negative skin friction or downdrag is a function of the relative displacement between the pile and the soil, the realistic determination of negative skin friction is dependent on the accuracy of measuring the pile and the soil settlements. Moreover, the negative skin friction is highly depends on the behavior of interface elements. Since the settlement of the ground surface due to construction of embankment is very large, the negative skin friction can be rapidly developed with in a short period of time. Axial load distribution along the pile shaft is shown in Fig. 2.3. They suggested that in order to minimize the negative skin friction, piles may be driven few weeks, or a month later after the surcharge load is applied on the ground surface.

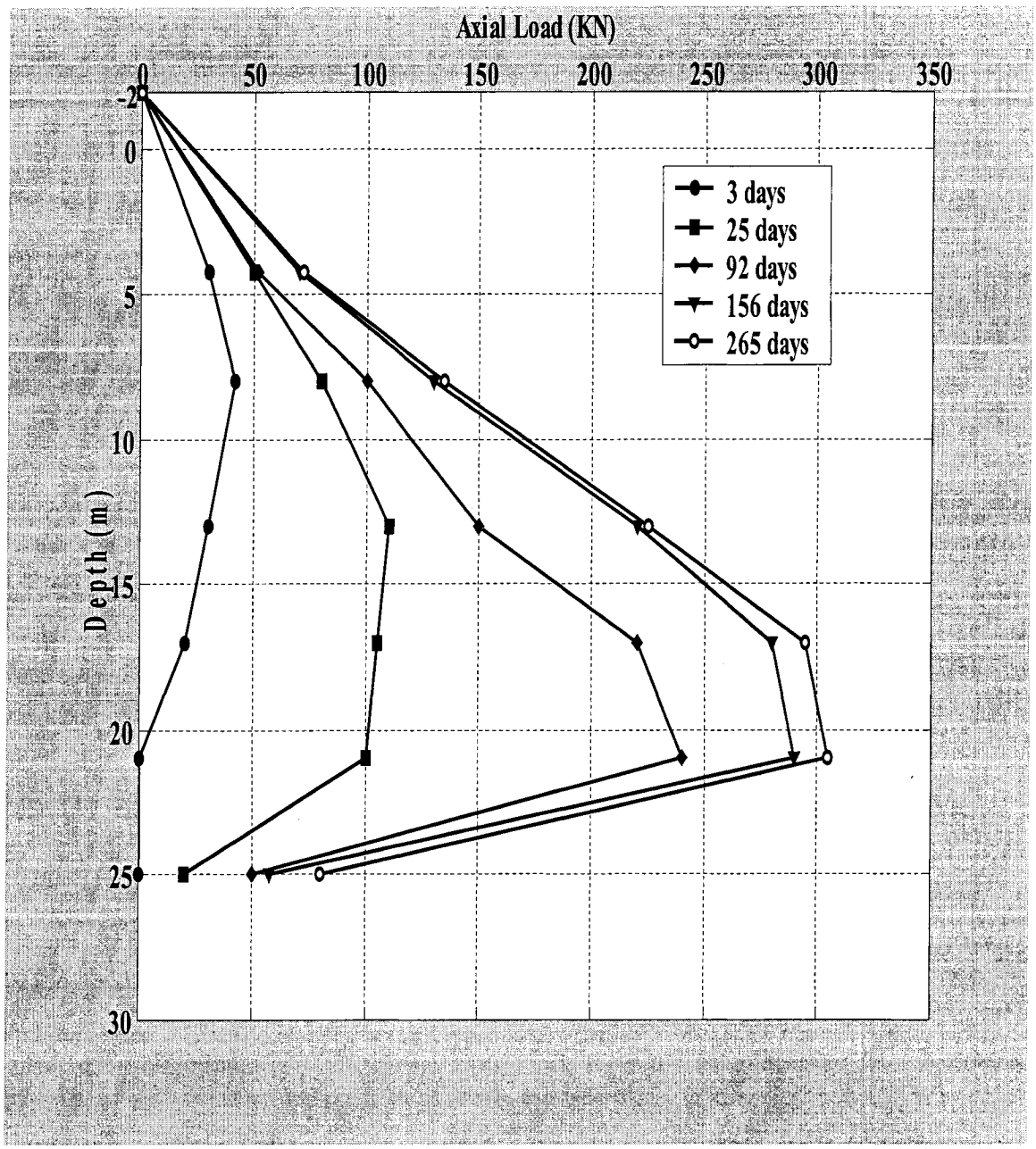

Fig. 2.3 Axial load distribution along the pile's shaft (After Indraratna et al, 1992)

C. Y. Lee (1993) presented a simplified hybrid load-transfer approach for analyzing the response of pile groups under negative skin friction. The response of single piles was carried out by a discrete- element approach while the interaction effect between piles in a group was approximated by a modified form of Midlin's (1936) analytical point–load solution. The piles were assumed to be surrounded in a consolidating soil layer and bearing on a stiffer stratum. A simple hyperbolic soil model characterized the pile-soil interface. The pile shaft for a single pile was discretized into discrete elements and the relative incremental settlement of the shaft elements subjected to uniform distributed shaft loads was approximated as follows.

$$\Delta w_s - \Delta w_c = \frac{\Delta P_s}{2\Pi G_t L}\left[In\frac{(r_m - \alpha_s)}{(r - \alpha_s)} + \frac{\alpha_s (r_m - r)}{(r_m - r)(r - \alpha_s)} \right] \quad \text{..... (2.12)}$$

$$\alpha_s = \frac{P_s r R_h}{P_{sf}}$$

Where, Δw_s is the incremental shaft settlement; Δw_c is the incremental consolidation settlement; G_t is the initial tangent soil shear modulus at pile shaft; r_m is the maximum radius at which settlements in soil negligible; r is the pile radius; P_s is the current shaft load; P_{sf} limiting shaft load and R_h is the hyperbolic soil parameter.

The pile base was represented as rigid punching at the surface of infinite soil mass ignoring the shaft and the surrounding soil, the relative incremental settlement of the pile's tip is given as follows.

$$\Delta w_b - \Delta w_c = \frac{\Delta P_b (1 - \nu)}{4 G_{br} r (1 - \alpha_b)^2} \quad \text{.....(2.13)}$$

$$\alpha_b = \frac{P_b R_h}{P_{bf}}$$

Where, Δw_b is the incremental pile base settlement; ΔP_b is the incremental base load;

G_{br} is the initial tangent soil shear modulus at the pile base; P_b is the current base load and P_{bf} is the limiting pile base load. This load transfer approach showed that in the linear elastic response, the interaction between piles in a group reduces the downdrag loads and the pile head settlement when compared with single piles. The theoretical solutions indicated that the pile head settlement and the downdrag force were affected by the relative pile stiffness, relative bearing stratum stiffness, pile spacing and the number of piles in the group.

Matyas and Santamarina (1994) presented elastic–plastic closed form solution that allows an estimate of downdrag and the location of the neutral plane in terms of the most relevant parameters. The pile's shaft and the toe resistances are characterized through an elastic-plastic soil model. They assumed that the relative displacement profile Fig. 2.4 as linear with maximum displacement at the ground surface and decreasing with an increase of depth. They derived a simple expression to determine the location of neutral plane and the load at the location of neutral plane resulting from the downdrag forces and the applied load. These expressions are as follow.

$$\lambda = \frac{\sqrt{(\alpha-1)^2 + 8\psi(\alpha-1) + 8\psi^2\left(1 - \frac{\alpha}{F_s} - \frac{2\omega^2}{3}\right)} - (\alpha-1)}{4\psi} \quad \text{.....(2.14)}$$

$$\frac{F_n}{P_u} = \frac{1}{\alpha}\left(\lambda^2 - \lambda\omega + \frac{1}{3}\omega^2\right) + \frac{1}{F_s} \quad \text{.....(2.15)}$$

Where,

$$\lambda = \frac{\delta_h}{S} = \frac{L_{NP}}{L} \qquad S = \delta_h + \delta_t;$$

$$\psi = \frac{\delta_{ty}}{S}$$

$$\omega = \frac{\delta_{sy}}{S}$$

$$\alpha = \frac{P_u}{P_{su}} \qquad F_s = \frac{P_u}{P}$$

δ_h is the settlement of the pile head relative to ground surface and δ_t is the relative settlement of the pile toe. δ_{sy} is the displacement of the soil relative to the pile that is required to yield the shaft resistance and δ_{ty} is the displacement that yields the toe resistance.

From the above expressions they concluded that conventional rigid-plastic models could overestimate the value of maximum axial load by 50%, possibly more and over predict the depth of the neutral plane.

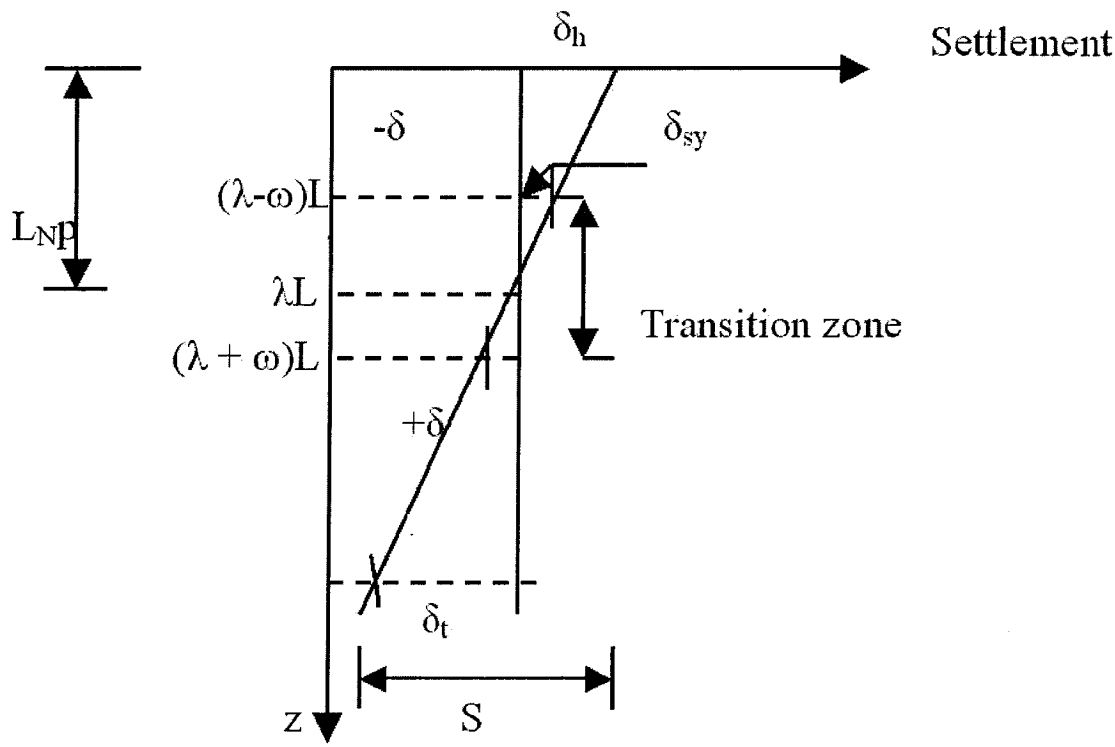

Fig. 2.4 Elastic-Plastic model (After Matyas and Santamarina, 1994)

Briaud et al (1994) conducted a nonlinear three-dimensional analysis of downdrag on group piles using a numerical analysis and an analytical study. The case of single pile and subsequently the response of group actions were analyzed with the aid of a three-dimensional nonlinear finite element approach.

They assumed that during the settlement of the soil layer the shear stresses in the soil, close to the pile shaft are fully mobilized since the relative movement between the soil and the pile is very large. For this reason, a portion of soil weight will be carried by the pile and consequently vertical effective stress will be decreased from $\sigma'(z)$ to $\sigma'(z, r)$ near to the pile (Fig. 2.5).

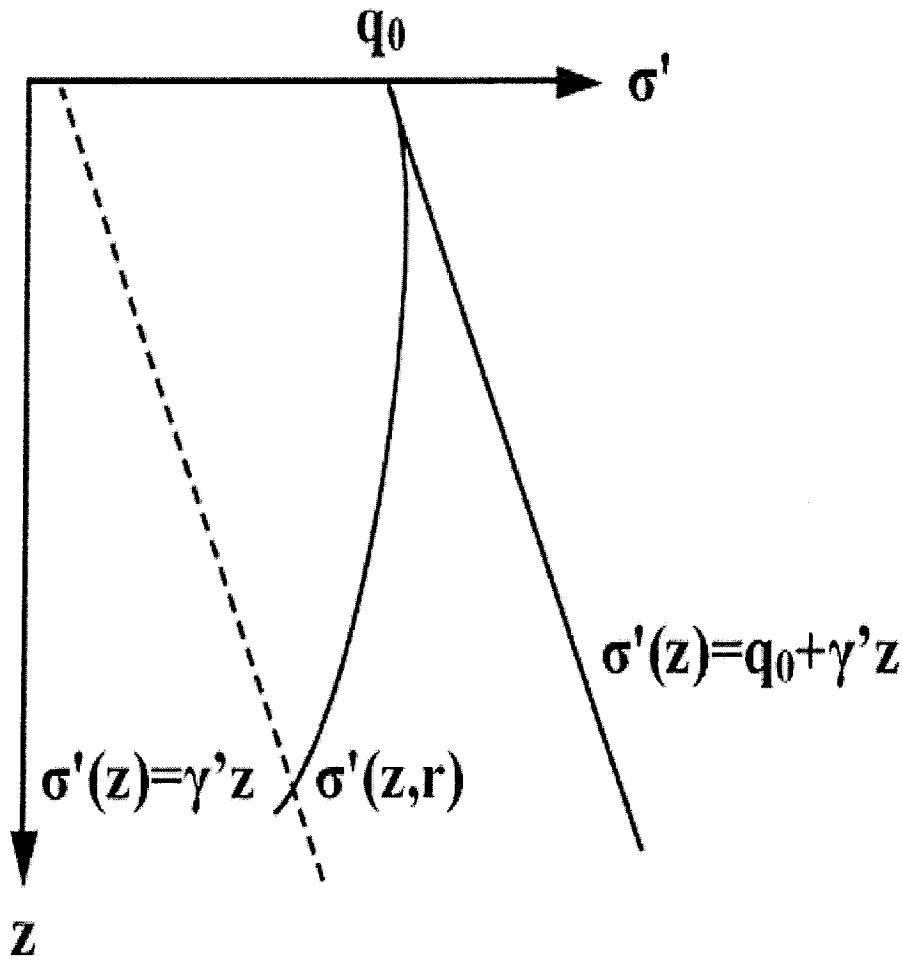

Fig. 2.5 Vertical effective stress near the pile's shaft (After Briaud et al, 1994)

Furthermore, they carried out parametric study for different end bearing conditions, cap rigidity, soil model and spacing between piles. Based on the results attained, they proposed a method to design groups of 9 to 25 piles with spacing to diameter ratios varying from 2.5 to 5.0 for downdrag. They concluded that the downdarg force on a pile group is much less then the downdrag on a single pile, the neutral plane for the group can be taken at the pile's tip for piles bearing on a perfectly rigid base, and for frictional piles

with no end bearing approximately equal to 75% of the length of the group for the corner and perimeter pile but at the tip for interior pile.

Wong and Teh (1995) presented a simplified numerical procedure for the analysis of the negative skin friction on piles in a layered soil. Their intention was to capture the complex phenomenon of the pile-soil interaction. They modeled the pile-soil interface as a hyperbolic soil springs in a manner similar to the load-transfer method. A pile embedded in a layered soil undergoing consolidation settlement (Fig. 2.6) was discretized into a finite number of cylindrical bar elements. The load-displacement behavior of the pile was presented by the following equation.

$$[K_p]\{w_p\} = \{P\} \quad \text{.....} \quad (2.16)$$

Where, K_p is pile stiffness matrix; w_p is the nodal displacement vector and the P is the nodal load vector. If there is no applied load, $\{P\}$ is the only load that caused relative displacement between the pile and the surrounding soil. The soil spring at the pile shaft is represented by the following hyperbolic equation.

$$P_i = w_i \Big/ \left(\frac{1}{K_{si}} + R_h \frac{w_i}{P_{ui}} \right) \quad \text{.....} \quad (2.17)$$

Where, K_{si} is the initial tangent of the hyperbolic curve, R_h is a hyperbolic constant, w_i is the relative pile-soil displacement, and P_{ui} is the maximum allowable nodal load. The hyperbolic soil spring constants are the function of the soil stiffness and the interface shear strength. The soil parameters required for this numerical procedure are the unit skin friction at the interface, soil shear modulus, Poisson ratio, and ultimate end bearing

capacity. In order to determine these input parameters Wong and Teh (1995) established a framework from the conventional soil test data.

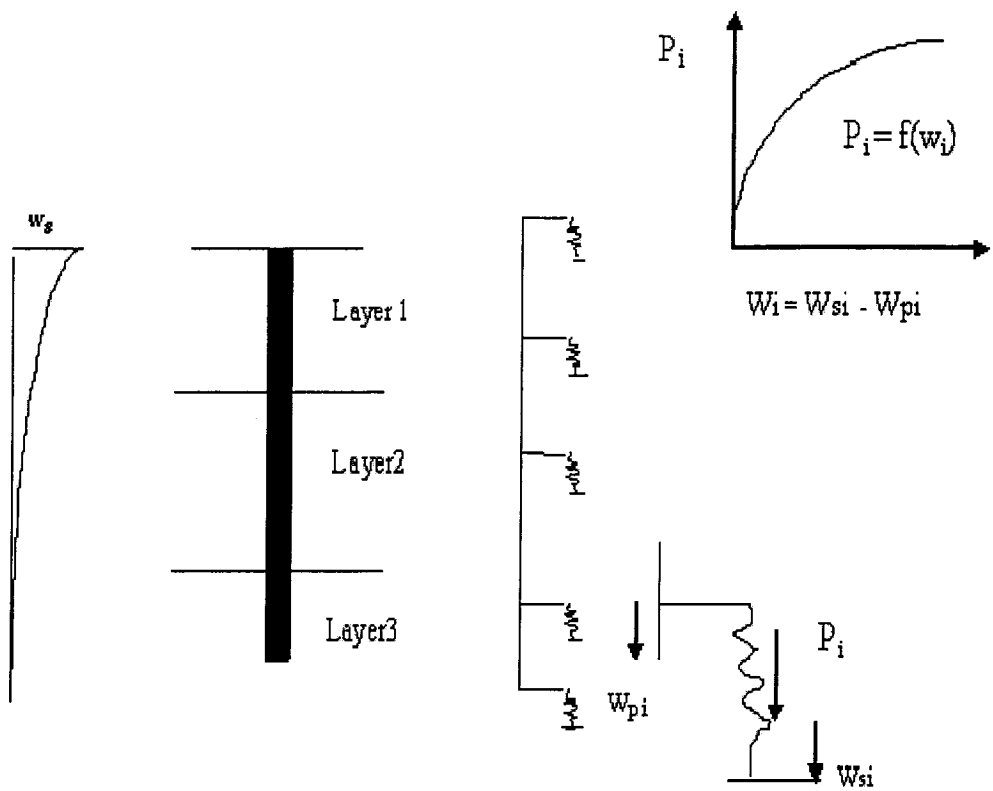

Fig. 2.6 Pile in layered soil (After Wong and Teh, 1995)

Chow et al (1996) reported a simplified method for the analysis of socketed pile groups subjected to negative skin friction. Piles were modeled using discrete elements with an axial mode of deformation. The soil behavior is modeled using a hybrid approach

in which soil response at the individual pile is modeled using the subgrade reaction method while pile-soil interaction is determined using the elastic theory.

The main difference between the methods lies in the manner in which pile-soil–pile interaction is determined. The accuracy of the methods is evaluated by comprehensive comparisons with more rigorous theoretical solutions. It is concluded that for practical pile groups, the layer model can give reasonable solutions provided the socket is not too deep.

Poorooshasb et al (1996) proposed a numerical scheme to evaluate the magnitude and form of the negative skin friction on piles. They studied the case of a single pile of circular cross section considering an axisymmetric problem with a surcharge pressure on the underlying clay layers. The governing equation of the problem is

$$\frac{\partial w}{\partial z}+f(z)\int_0^{\varepsilon}\left[g(\varepsilon)\frac{\partial^2 w(r,\varepsilon)}{\partial r^2}+\frac{1}{r}\frac{\partial w(r,\varepsilon)}{\partial r}\right]d\varepsilon-f(z)p_0=0 \quad \text{.....} \quad (2.16)$$

Where,

w is displacement in the z direction.

f(z) is a soil parameter similar to the inverse of Young's modulus.

g(z) is a soil parameter same as shear modulus G.

r is the radial co-ordinate.

p_0 is a constant equal to the value of surcharge on the ground surface.

This numerical scheme is capable of handling complicated situation, such as the non-linearity of the material, radial non-homogeneity and the soil stratification. It showed that

the depth of fill does not have greater influence over the neutral depth. But the bearing stratum of pile, particularly a strong bearing stratum has a significant influence over the depth of neutral depth. Moreover, it was mentioned that in case of pile group rests on bedrock, a substantial portion of the pile sustains very little, or no skin friction. The zone of negative skin friction is suggested to be at a depth of one third of the pile length, unless a very low angle of internal friction for the pile-soil interfaces.

Briaud et al (1997) investigated the case of negative skin friction on frictional and end bearing pile groups. They emphasized on quantifying the reduction of the downdrag load on the groups with a flexible pile cap. The case of single piles and the response of groups were analyzed by developing interaction factors obtained from a three dimensional non-linear finite element analysis. Based on few parametric studies, they reported that the downdarg force on piles in a group is much less than the downdrag on a single pile and is highly influenced by the group spacing, number of piles in the group, and the relative position of the piles in a group. Based on the results of their study, a simple method was recommended for square groups of 9 to 25 piles with spacing to diameter ratios of 2.5.

Shen and Teh (2002) presented a rational solution for the analysis of downdrag forces of pile groups. The theoretical load transfer curves were used to describe the soil load-displacement relationship. The principal of minimum potential energy was applied to determine the response of pile groups. The initial stress technique was adopted for the

slippage at the pile-soil interface. In this analysis, the soil load–displacement relationship had been presented by the following equations

$$\tau_z = [k]\{w_z\} \quad \text{.....} \quad (2.19)$$

$$\sigma_l = [k_b]\{w_l\} \quad \text{.....} \quad (2.20)$$

Where τ_z and σ_l are the stresses at the pile shaft and the base; w_z and w_l are the displacements at the pile shaft and base; k and k_b are the soil stiffness matrices for the pile cap and the pile base.

They assumed that soil movement decreases linearly with depth; maximum at the pile head to zero at the pile toe. The soil stiffness was assumed to increase linearly with depth along the pile's shaft.

Ng and Lee (2004) presented two-dimensional axisymmetric and three-dimensional numerical models to examine the development of the downdrag force on single pile and pile groups in soil subjected to consolidation. They performed elastic no–slippage and elastic-plastic slippage analysis at the pile soil interface. According to their results, in case of a single pile, the downdrag forces computed from no slippage elastic analysis was 8 to 14 times greater than the computed downdrag from elasto-plastic analysis.

The parametric study was performed considering different pile length and pile group. The ground water table was taken to be at the clay surface. The development of negative skin friction was introduced by applying a uniform surface loading on the top the clay surface. All analyses were carried out under uncoupled and drained conditions.

They concluded that the relative pile to clay stiffness and the relative stiffness of the bearing stratum to the consolidating soil affect the developed downdrag force on a single pile. Furthermore, the downdrag force on single pile is reduced nonlinearly with an increase in the relative bearing stratum stiffness.

Hanna and Sharif (2006) conducted a study on piles driven into clay and subjected to indirect loading through the surcharge applied symmetrically on the surrounding area. The study was based on a numerical model using finite element technique and the soil was assumed to follow a linear elastic-perfectly plastic stress-strain relationship, which is defined by Mohr-Coulomb failure criterion. The pile's material was assumed to behave as linear elastic. The model was used to generate a wide range of data to investigate the location of the neutral plane and drag forces acting on the pile. Based on the results obtained, they performed a parametric study on angle of shearing resistance, surcharge factor, safety factor, and pile length to diameter ratio.

They concluded that negative skin friction is developed on the pile's shaft during the undrained period and continues to exist until the consolidation of the surrounding soil is completed under surcharge loads. Negative skin friction is induced from the top of the pile and extends progressively downward, until it reaches a maximum value at an intermediate depth. Then it decreases up to the level of the neutral plane. They proposed that the depth of neutral plane increases due to a decrease of the surcharge factor and due to an increase of the safety factor and the pile length to diameter ratio. Further, they presented a design procedure to predict the allowable load of a single pile in clay subjected to direct and indirect loads.

2.3 Discussion

A significant amount of research has been carried out to investigate the development of negative skin friction on individual piles and pile groups in the last few decades. Some researcher conducted field tests to study the real scenario in soils due to surcharge loading and gathered information related to soil settlement, excess pore pressure, pile behavior and capacity. However, field tests are limited to the soil condition of the site where the tests were carried out. Most of the numerical analyses reported were based on simplifying assumptions, such as linear material deformation, single material domain, undrained and, or drained test for skin friction distribution. Few tests were carried out for time dependent distribution of skin friction and uncoupled consolidation analysis for settlement of soils adjacent to pile surface. Due to the consideration of these simplifying assumptions, prediction of the negative skin friction and the location of neutral plane were not very effective where different layer of soils exist.

CHAPTER 3

NUMERICAL MODEL

3.1 General

Finite element technique is a reliable tool in the field of geotechnical engineering to solve complex soil-structure interactions problems. The case of single piles or group of piles subjected to direct and indirect loading is no exception.

3.2 The Program

Present study adopted the program (PLAXIS), which is a program based on the finite element technique. In this program, the calculation process is divided into a number of calculation phases, in which loads are subdivided into increments and the soil stiffness are adjusted accordingly. The program is capable to perform different types of finite element calculations; such as Undrained, drained, consolidation, safety and dynamic analysis and axisymmetric and two and three dimensional method of analyses.

3.3 The Numerical Model

Axisymmetric model is suitable for the case of a single pile with uniform radial cross section and loading scheme on the central axis and the surrounding area. The deformation and stresses are identical in any radial direction in the axisymmetric analysis. The "x" co-ordinate represents the radial direction while the "y" co-ordinate corresponds to the vertical line of symmetry.

3.3.1 The Geometry of the model

The width of the mesh was taken as 25 times the diameter of the pile, or 0.6 times the length of the pile whichever is larger and the length of the mesh was assumed as 1.7 times the length of the pile. Preliminary test proved that these values do not produce any boundary effects. Fig. 3.1 presents the geometry of the numerical model.

3.3 .2 The Boundary condition

The bottom boundary line of the mesh is considered as fixed both in lateral and in longitudinal (depth) direction (i.e No displacement is permitted at the bottom of the mesh). The left and the right boundaries are only restrained in the lateral direction (i. e in 'x 'direction) and free in the longitudinal direction (i.e in 'y' direction).

3.3.3 Mesh Generation

15 nodes triangular elements are used to generate the mesh for the proposed numerical model. Fig. 3.2 presents mesh generation. A 15 nodes triangular element provides a fourth order interpolation for displacements and the numerical integration involves twelve gauss points (stress points). Moreover, a 15 nodes triangular element is very accurate to produce high quality stress results although it consumes relatively high memory and according computing time. Moreover, the mesh is refined in the vicinity of pile to get more accurate results from the analysis. Fig. 3.3 shows the 15 nodes triangular elements with 12 stress points.

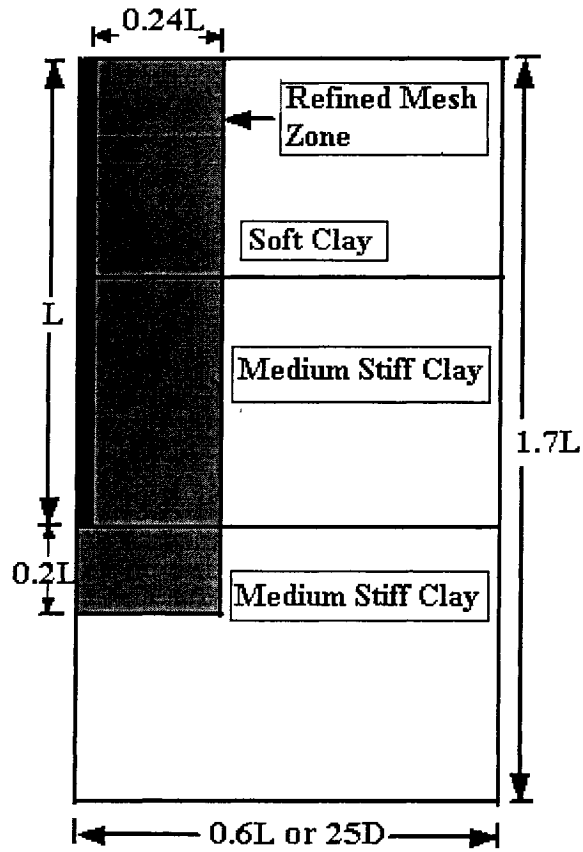

Fig. 3.1 Geometry of the finite element mesh

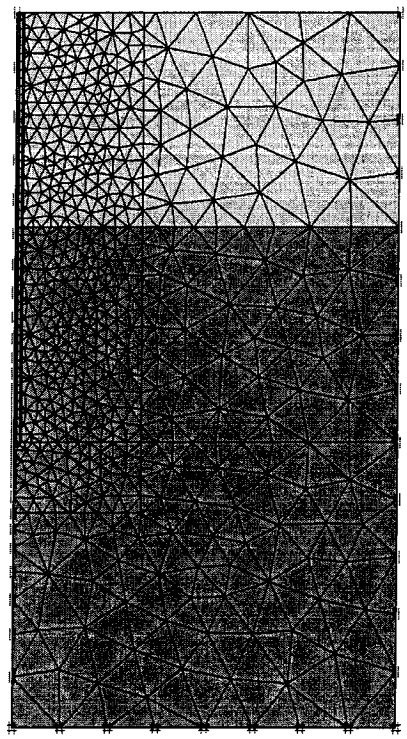

Fig. 3.2 Generation of mesh in the geometric domain

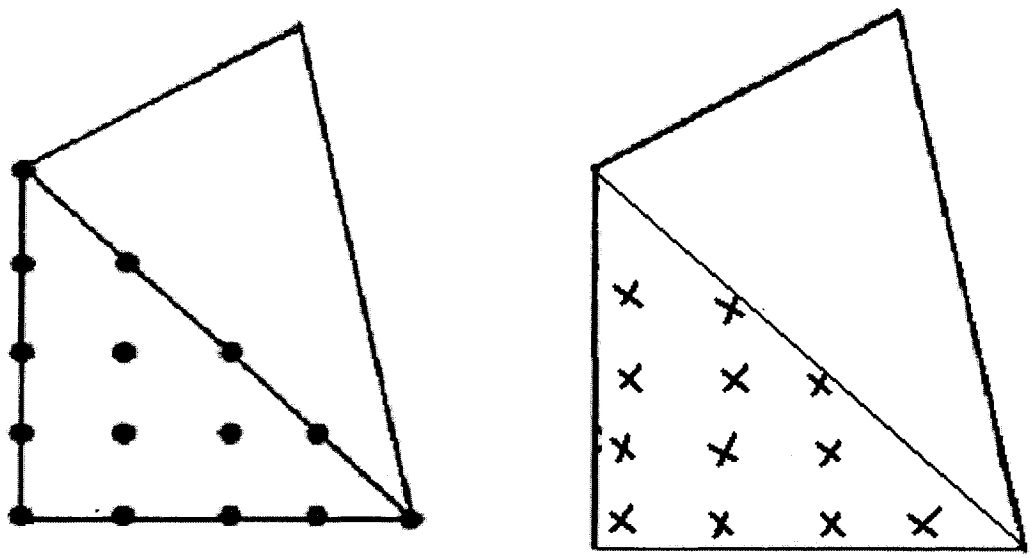

(a) Position of nodes **(b) 12 stress points in element.**

Fig. 3.3 15 nodes triangular soil element

3.3.4 Pile-Soil Interface Elements

The pile and the soil interface are constituted with interface elements. The interface elements properties are associated with the corresponding set of soil material properties. For 15 nodes triangular elements, the interface elements are designed with 10 nodes and 5 stress points (Fig.3.4). The interface elements have assigned a "virtual thickness" which is an imaginary dimension used to define the material properties of the interface elements. The virtual thicknesses of the interface elements are calculated using a virtual thickness factor time the average element size. The default value of this factor is "0.1".

Stiffness matrix of interface elements is obtained by means of Newton Cotes integration. An elastic-plastic model is assumed to describe the behavior of the interface of the soil-structure interaction. A small displacement was observed followed by permanent slip at the interface elements during the elastic and plastic stages respectively.

The strength properties of the interface elements are correlated with the strength properties of adjacent soil elements. A strength reduction factor is associated for the properties of soil. This reduction factor determines the properties of the interface elements based on the properties of corresponding soil layer.

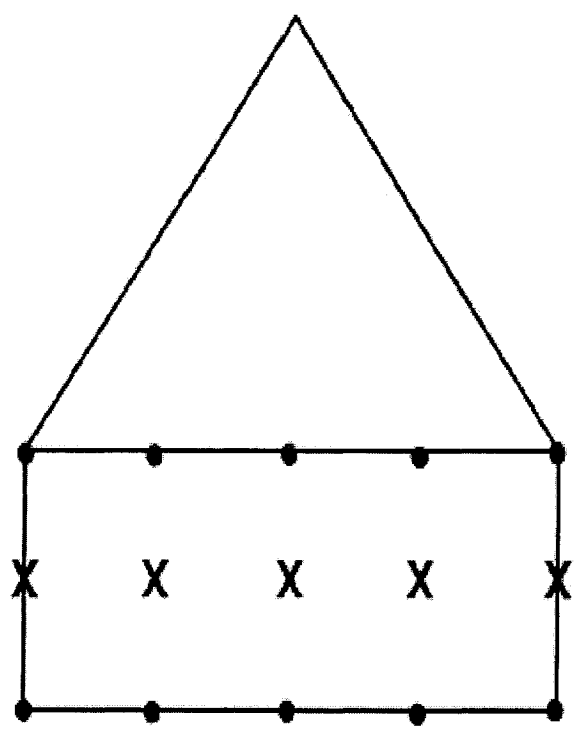

Fig. 3.4 10 Nodes interface element with 5 stress points and its connection to soil elements.

3.4 Soil Constitutive Model

The soil is assumed to behave as an elastic perfectly plastic material. A perfectly plastic model is a constitutive model with fixed yield surface based on model parameters. In elastic perfectly plastic material model strain and strain rates are decomposed into elastic and a plastic part. Hook's law is used to relate the stress field to the elastic strain. The plastic strain rates are proportional to the derivative of the yield function with respect to the stresses i.e the plastic strain rates can be represented as vectors perpendicular to the yield surface. However, this form of theory is an over prediction of dilatancy for Mohr – Coulomb yield function. Therefore, a plastic potential function is introduced with yield function .The basic parameters required for the elastic perfectly plastic model includes: Modulus of elasticity (E), Poisson ratio (υ), Cohesion (c'), angle of internal friction (ϕ'), and dilatancy angle (ψ). Fig. 3.5 presents typical elastic perfectly plastic model.

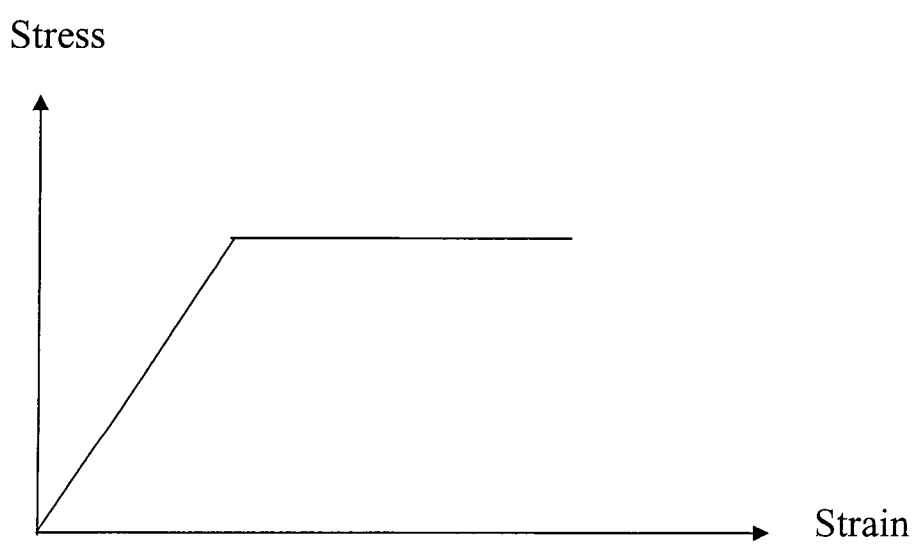

Fig. 3.5 Elastic perfectly plastic model

3.4.1 Material Properties

Two types of clay materials are adopted in this analysis. The upper layer was taken as a soft clay layer, while the lower layer was medium stiff clay, which is extended to an infinite depth. Length of the upper soft clay layer is variable in order to investigate stress distribution and settlement due to surcharge loading. The soil properties for different cohesion ratio are shown through Table 3.1 to Table 3.5. A circular concrete pile is used in this analysis whose tip is rest on the medium stiff clay layer. Properties of the pile material are shown in Table 3.6.

Soil Type	γ_{unsat} (kN/m^3)	γ_{sat} (kN/m^3)	c' (kPa)	ϕ'	E (kPa)	υ	k_x (m/day)	k_y (m/day)
Soft Clay	14	15.5	10	15	5000	0.2	8.0×10^{-4}	8.0×10^{-4}
Medium Stiff Clay	-	19	50	20	38000	0.25	4×10^{-4}	4×10^{-4}

Table 3.1 Properties of the clay used (Cohesion ratio 0.2)

Soil Type	γ_{unsat} (kN/m^3)	γ_{sat} (kN/m^3)	c' (kPa)	ϕ'	E (kPa)	υ	k_x (m/day)	k_y (m/day)
Soft Clay	14	15.5	15	15	6000	0.2	7.5×10^{-4}	7.5×10^{-4}
Medium Stiff Clay	-	19	50	20	38000	0.25	4.0×10^{-4}	4.0×10^{-4}

Table 3.2 Properties of the clay used (Cohesion ratio 0.3)

Soil Type	γ_{unsat} (kN/m^3)	γ_{sat} (kN/m^3)	c' (kPa)	ϕ'	E (kPa)	υ	k_x (m/day)	k_y (m/day)
Soft Clay	14.5	16	20	15	7000	0.2	7.0×10^{-4}	7.0×10^{-4}
Medium Stiff Clay	-	19	50	20	38000	0.25	4.0×10^{-4}	4.0×10^{-4}

Table 3.3 Properties of the clay used (Cohesion ratio 0.4)

Soil Type	γ_{unsat} (kN/m^3)	γ_{sat} (kN/m^3)	c' (kPa)	ϕ'	E (kPa)	υ	k_x (m/day)	k_y (m/day)
Soft Clay	14.5	16	25	15	8500	0.2	6.5×10^{-4}	6.5×10^{-4}
Medium Stiff Clay	-	19	50	20	38000	0.25	4.0×10^{-4}	4.0×10^{-4}

Table 3.4 Properties of the clay used (Cohesion ratio 0.5)

Soil Type	γ_{unsat} (kN/m^3)	γ_{sat} (kN/m^3)	c' (kPa)	ϕ'	E (kPa)	υ	k_x (m/day)	k_y (m/day)
Soft Clay	15	16.5	30	15	10000	0.2	6.0×10^{-4}	6.0×10^{-4}
Medium Stiff Clay	-	19	50	20	38000	0.25	4.0×10^{-4}	4.0×10^{-4}

Table 3.5 Properties of the clay used (Cohesion ratio 0.6)

Material	Length (m)	Diameter (mm)	γ (kN/m^3)	E (kPa)	υ
Pile	30	500	24	30,000000	0.3

Table 3.6 Properties of the Pile material.

3.5 Coupled Consolidation Analysis

In uncoupled analysis the fluid flow and solid deformation analysis carried out independently. The change in the pore pressure at a particular time due to dissipation of the excess pore pressure is calculated separately and used as an applied load for deformation analysis of the porous media. However, coupling between solid to fluid occurs in the underground formation where load is applied, or the change in the fluid pressure will change the volume of the porous material. When loads are applied, a significant amount of pore pressure is generated in fluid-saturated porous material. Changes in the fluid pressure cause a time dependent volume change in solid media. This type of two ways coupling is called coupled.

A coupled consolidation analysis is performed to calculate the time dependent development or dissipation of excess pore pressures in water-saturated clay-type soils. Biot's theory for consolidation, Darcy's law for fluid flow, and elastic behavior of soil particle are taken into consideration for the consolidation analysis. Ground water level was assumed to be located 2 m below the ground surface. Excess pore pressure generated

during the undrained period is considered in the consolidation analysis. Therefore, the modeled developed should be capable to analyze consolidation behavior without any additional loading after the undrained period. For consolidation analysis automatic time stepping procedure is adopted. This procedure chooses proper time steps automatically for the consolidation analysis.

3.5.1 Coupled Consolidation Model

The radial direction is considerate as 'x' direction and the axial line of symmetry as 'y' direction in this model. The two dimensional equilibrium equations can be written as follows.

$$\frac{\partial \sigma_x}{\partial x} + \frac{\partial \tau_{xy}}{\partial y} + \frac{\partial p}{\partial x} = 0 \quad \text{.....(3.2)}$$

$$\frac{\partial \sigma_y}{\partial y} + \frac{\partial \tau_{xy}}{\partial x} + \frac{\partial p}{\partial y} = 0 \quad \text{.....(3.3)}$$

Where, σ_x, σ_y are the effective normal stress and τ_{xy} is the shear stress. p is the excess pore pressure and the continuity equation can be written as following:

$$\frac{\partial q_x}{\partial x} + \frac{\partial q_y}{\partial y} + \frac{\partial}{\partial t}\left(\frac{\partial u}{\partial x} + \frac{\partial v}{\partial y}\right) = 0 \quad \text{.....(3.4)}$$

Where, q_x and q_y are the flow per unit volume of an element and u and v are the displacement of the element.

3.5.2 Finite Element Discretization

The above equilibrium equation can be discretized in the following form.

$$\mathbf{K}dr + \mathbf{C}dp = dF \quad \text{.....(3.5)}$$

Where, **K** is the stiffness matrix, **C** is the coupling matrix, **p** is the excess pore pressure vector and **F** is the increment load vector.

Thus:

$$\mathbf{K} = \int \mathbf{B}^{\mathbf{T}} \mathbf{E}_{\mathbf{M}} \mathbf{B}\, dV \quad \dots\dots\dots\dots (3.6)$$

Where, B is the element's strain-displacement matrix, *d*V is the intregration over the volume.

$$\mathbf{C} = \int \mathbf{B}^{\mathbf{T}} \mathbf{MN}\, d\mathrm{V} \quad \dots\dots\dots\dots (3.7)$$

M is the vector containing unity terms for normal stress components and zero terms for shear stress component, N is the matrix of shape function.

$$\mathbf{M} = [1 \quad 1 \quad 1 \quad 0 \quad 0 \quad 0]^{\mathrm{T}}$$

$$d\mathbf{F} = \int \mathbf{N}^T dfdv + \int \mathbf{N}^T dtds \quad \dots\dots\dots\dots (3.8)$$

Where f is the body forces and t is the surface tractions, *ds* is surface integral.

The continuity equation can be written as follows.

$$\nabla^T \mathbf{k}\ \nabla\left(y - \frac{p_s}{\gamma_w} - \frac{p_e}{\gamma_w}\right) - \mathbf{M}^T \frac{\partial \varepsilon}{\partial t} + \frac{n}{K_w}\frac{\partial p_e}{\partial t} = 0 \quad \dots\dots\dots\dots (3.9)$$

Where, **k** is the permeability matrix.

$$\mathbf{k} = \begin{bmatrix} \mathrm{k_x} & 0 \\ 0 & \mathrm{k_y} \end{bmatrix} \quad \dots\dots\dots\dots (3.10)$$

p_s and p_e are the steady state and excess pore pressure, n is the porosity of soil and K_w is the bulk modulus of the pore water .

For the case of steady state of pore pressure

$$\nabla^T \mathbf{k}\ \nabla\left(y - \frac{p_s}{\gamma_w} - \right) = 0 \quad \text{.....(3.11)}$$

Therefore, continuity equation takes the following form.

$$\nabla^T \mathbf{k}\ \nabla\left(\frac{p_e}{\gamma_w}\right) + \mathbf{M}^T \frac{\partial \varepsilon}{\partial t} - \frac{n}{K_w}\frac{\partial p_e}{\partial t} = 0 \quad \text{.....(3.12)}$$

Applying the finite element discretization using "Galerkin" procedure and incorporating the prescribed boundary condition, thus

$$-\mathbf{Hp} + \mathbf{C}^{\mathrm{T}} \frac{d\mathbf{r}}{\mathrm{dt}} - \mathbf{S}\frac{\mathrm{d}\mathbf{p}}{\mathrm{dt}} = \mathbf{q} \quad \text{.....(3.13)}$$

Where,

$$\mathbf{H} = \int (\nabla \mathbf{N})^T \mathbf{k} \nabla \mathbf{N} / \gamma_w dV$$

$$\mathbf{S} = \frac{n}{K_w} N^T N dV$$

q is a vector prescribed the outflow at the boundary, q is equal to zero at the boundary. The equilibrium and continuity equation can be combined in the following matrix form.

$$\begin{bmatrix} \mathbf{K} & \mathbf{C} \\ \mathbf{C}^{\mathrm{T}} & -\mathbf{S} \end{bmatrix} \begin{bmatrix} \frac{d\mathbf{r}}{\mathrm{dt}} \\ \frac{d\mathbf{p}}{\mathrm{dt}} \end{bmatrix} = \begin{bmatrix} 0 & 0 \\ 0 & \mathbf{H} \end{bmatrix} \begin{bmatrix} \mathbf{r} \\ \mathbf{p} \end{bmatrix} + \begin{bmatrix} \frac{d\mathbf{F}}{dt} \\ \mathbf{q_n} \end{bmatrix} \quad \text{.....(3.14)}$$

An integration procedure is used to solve the above equation.

3.5.3 Drainage Boundary

The top and bottom of the soft clay layer are adopted for drainage of excess pore water during the consolidation process. However, the pile-soil interface boundary is closed for water flowing into the pile.

3.6 Model Validation

Finite element analysis is performed to compare the downdrag forces, settlements and axial forces on piles due to surcharge loading. Analysis was carried out according to the actual field data available in the literature. The comparison of different field tests with the results predicted by the present numerical model is provided in the following section.

3.6.1 Field Test on Bangkok Clay

Indraratna et al (1992) carried out a field investigation on the downdrag load due to a surcharge load on driven piles in Bangkok clay. Two hollow test piles of prestressed, precast and concrete type were driven at a depth of 27 meters below ground. 2m fill was placed to investigate the downdrag load generated on the piles due to the settlement of the underneath soils. Water table was reported at 1.5 m to 2m a below ground. The soil properties are given in Table 3.7. A time dependent settlement analysis was carried out to investigate the settlement of clay layers due to surcharge loading. It has been observed that no excess pore pressure was noted after 265 days. According to the field observation, the neutral plane (zero stress) after 265 days of consolidation time was located at 20 m below the ground surface and 280 mm settlement was found during this time. A comparison between the measured settlement and the predicted values by the present

numerical model is shown in Fig. 3.6. In addition; skin friction distribution is compared with numerical model analysis which is shown in Fig. 3.7.

Depth (m)	γ **(kN/M3)**	**Es (kPa)**	Υ	**c' (kPa)**	ϕ'	Kx, Ky (m/day)
0 to 4	17	4900	0.2	3	18	67.6×10^{-5}
4 to 10	15	5000	0.2	6	20	5.5×10^{-5}
10 to 20	17	5000	0.2	15	22	2.63×10^{-5}
20 to 24	19	6500	0.3	6	23	3.72×10^{-5}
24 to 28	19.5	28000	0.33	40	23	3.72×10^{-5}

Table 3.7 Properties of soil tested (After Indraratna et al, 1992)

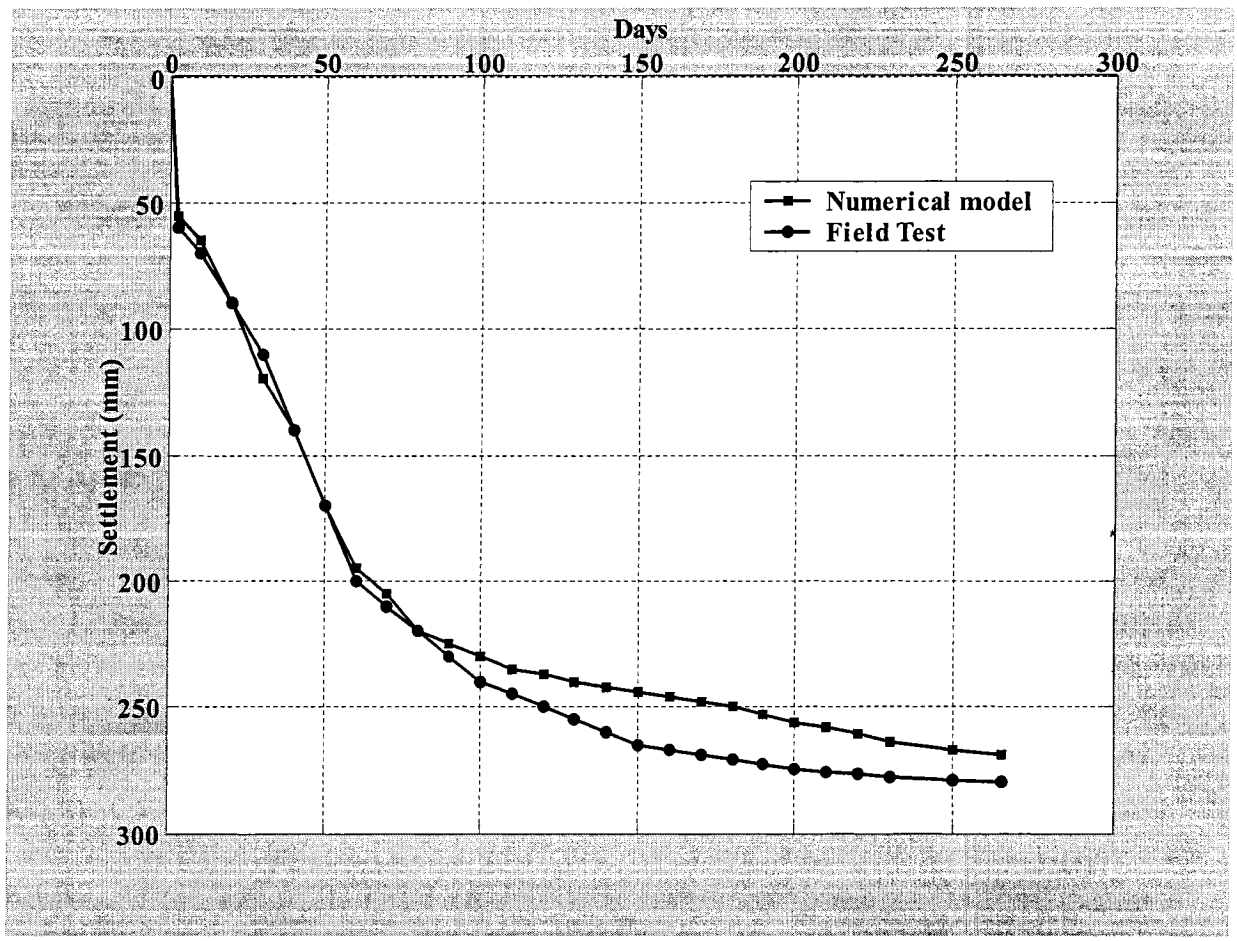

Fig. 3.6 Comparison between predicted and field measured values (Indraratna et al, 1992) of soil settlements.

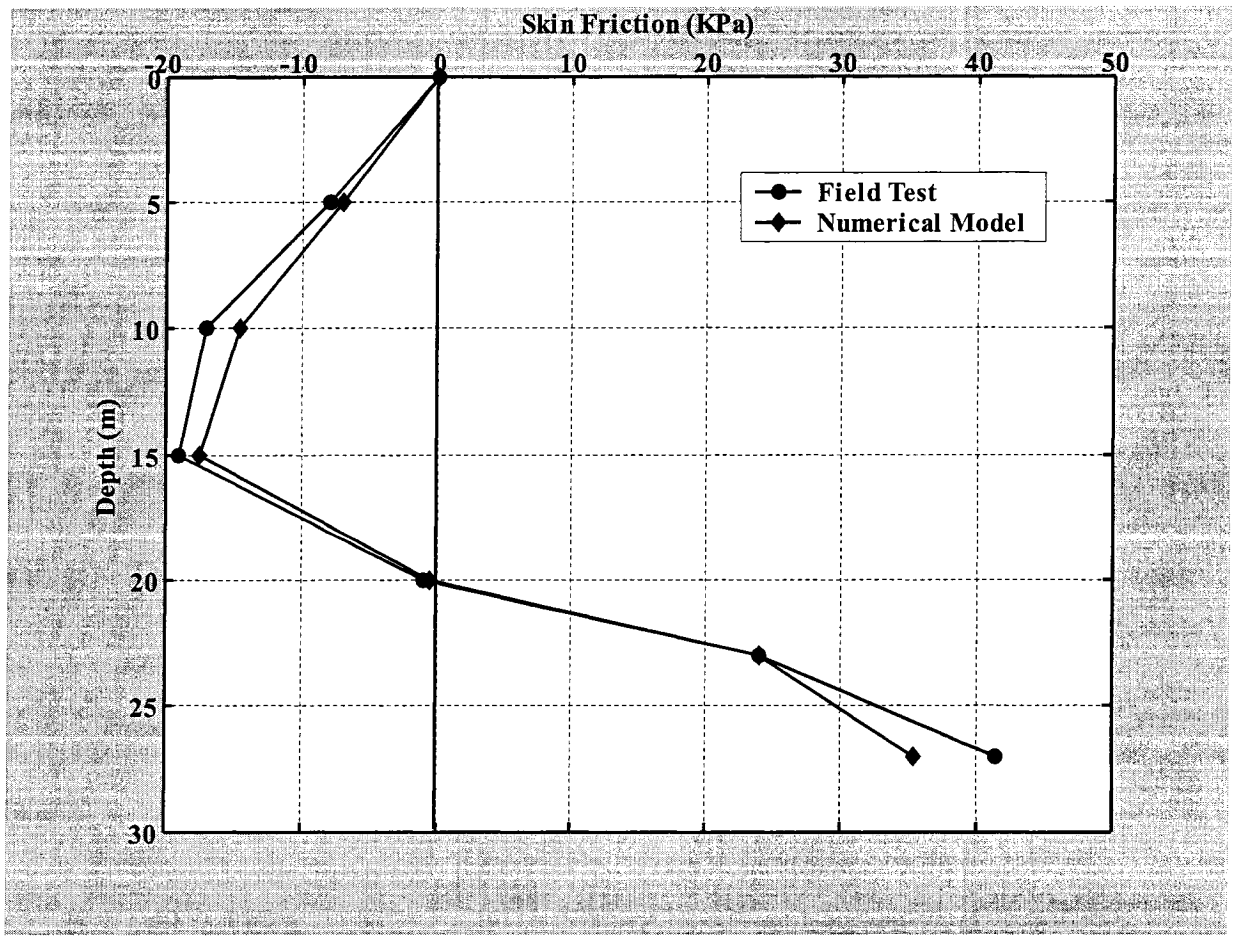

Fig. 3.7 Comparison between predicted and field measured values (Indraratna et al, 1992) of the skin friction.

3.6.2 Field Test in Tokyo, Japan

Endo et al (1969) reported a field test on three vertical and two battered piles for time dependent downdrag measurement at Fukagawa about 3 km west of down town Tokyo, Japan. Two of the three vertical piles were 43 m long with an outside diameter of 609.6 mm. A 43 m thick alluvium was deposited in a buried, which had been formed by an old river. This alluvium was deposited over diluvial sand. A silty sand layer of 7 m thick underlies a 2m fill. Below the silty sand layer a soft slit stratum containing sandy silt was

extended to a depth of 39 m, which was rest on a 4m thick hard silt layer. The bearing stratum of the pile was the diluvial sand layer. The water level was found at 1.5 below the surface. Fig.3.8 presents the soil profile together with the soil properties.

The rate of the settlement at the ground was recorded from June 1964 just after the piles were driven. The ground settlement was very large during the first four months and then gradually decreased. Measurement of the ground settlement was monitored until October 1967. It was found that the settlement occurred was about 130 mm after 672 days. Taking the data from the field measurement for soil properties, fill material properties, and rate of flow, the numerical model was adopted to perform the analysis and is compared the results with the field measurements. Fig. 3.9 presents the results of the numerical model together with the field settlement after 672 days.

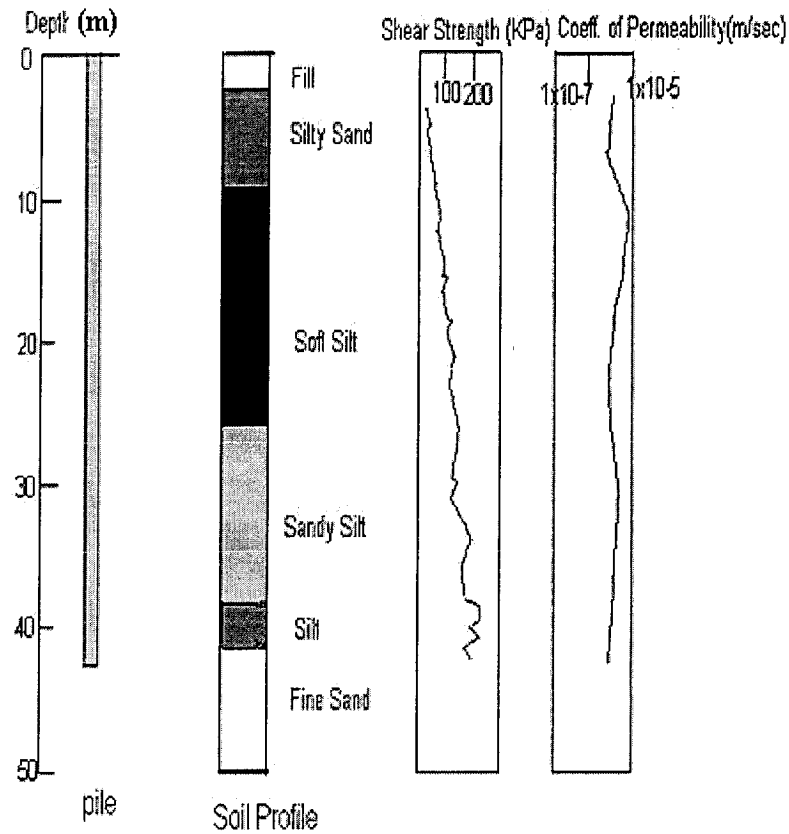

Fig. 3.8 Soil profile (After Endo et al, 1969)

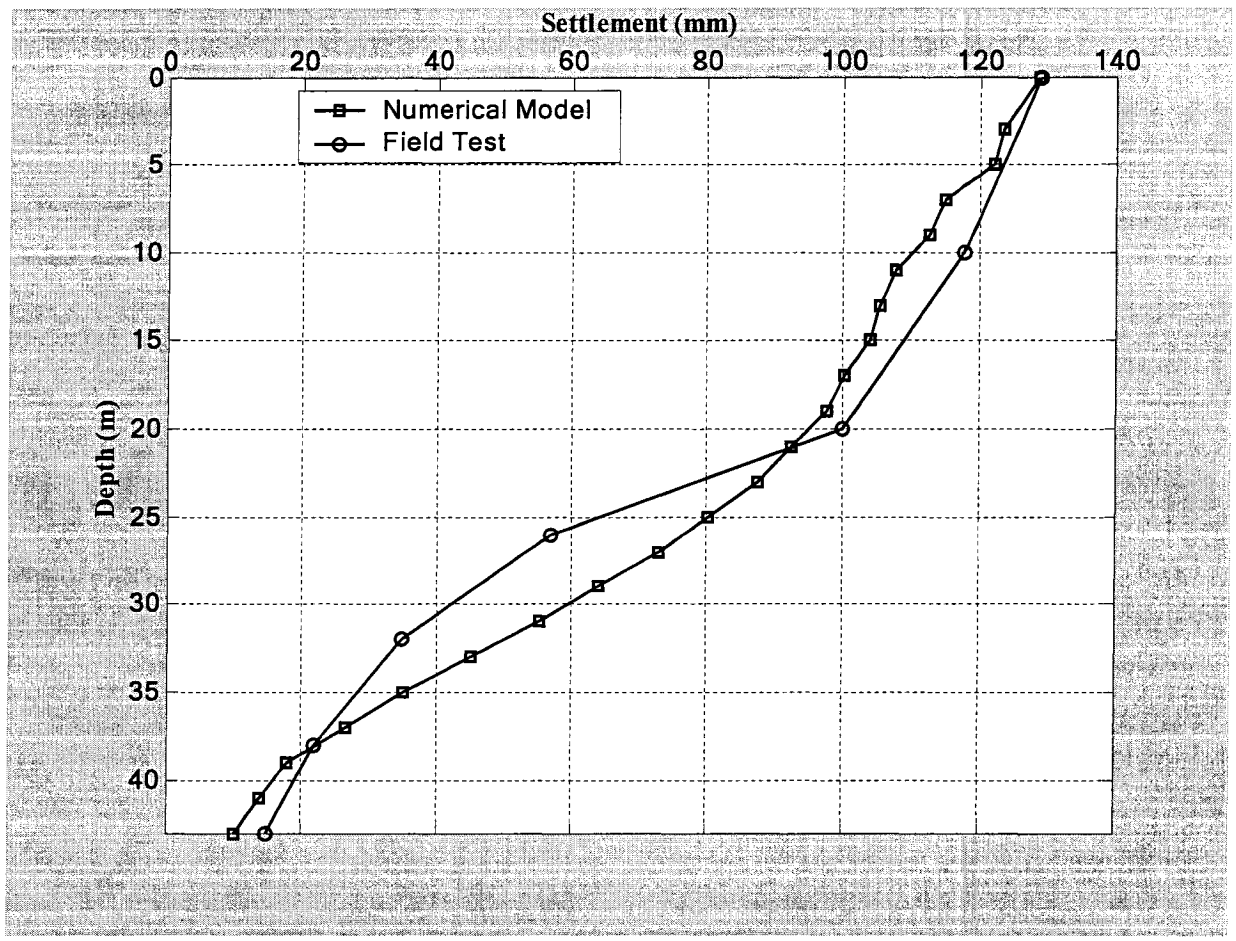

Fig. 3.9 Comparison between predicted and field measured values (Endo et al, 1969) of the soil settlements.

3.6.3 Field Test in Melbourne, Australia

Walker and Darvall (1973) carried out a field test to investigate the downdrag of a steel pipe pile in Melbourne, Australia. The length of the steel pipe pile was 34 m long with an external diameter of 760 mm. A test embankment of 3m heights was constructed after the pile was driven. An existing fill of 4m thick was found laid over 5m medium fine sand layers. A 15.5 m thick firm silty clay layer was found below the medium fine sand layer. A sandy silt layer of 3m thick was existed below silty clay layer. The sandy silt layer was

rest on dense sand and gravel, which was extended to a depth of 35m. The ground water level was found 1.5m below the ground surface.

The pile was monitored for 8-month period and the settlement was recorded regularly. The consolidation process was completed within the first four months. During this period the ground settled about 29 mm. The properties of fill and sand layers were measured from SPT *N*-values field tests. Fig.3.10 presents the soil profile together with shear strength. Using the measured properties of different soil layer, the present numerical model was used to compare with the field measurement. The soil settlement from numerical model is compared with field measured settlement which is shown in Fig. 3.11.

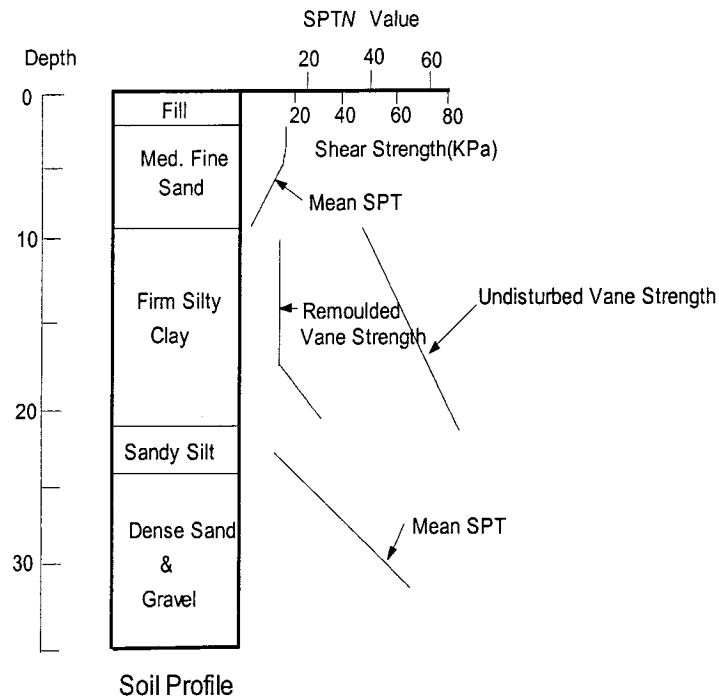

Fig. 3.10 Soil profile (After Walker and Darvall, 1973)

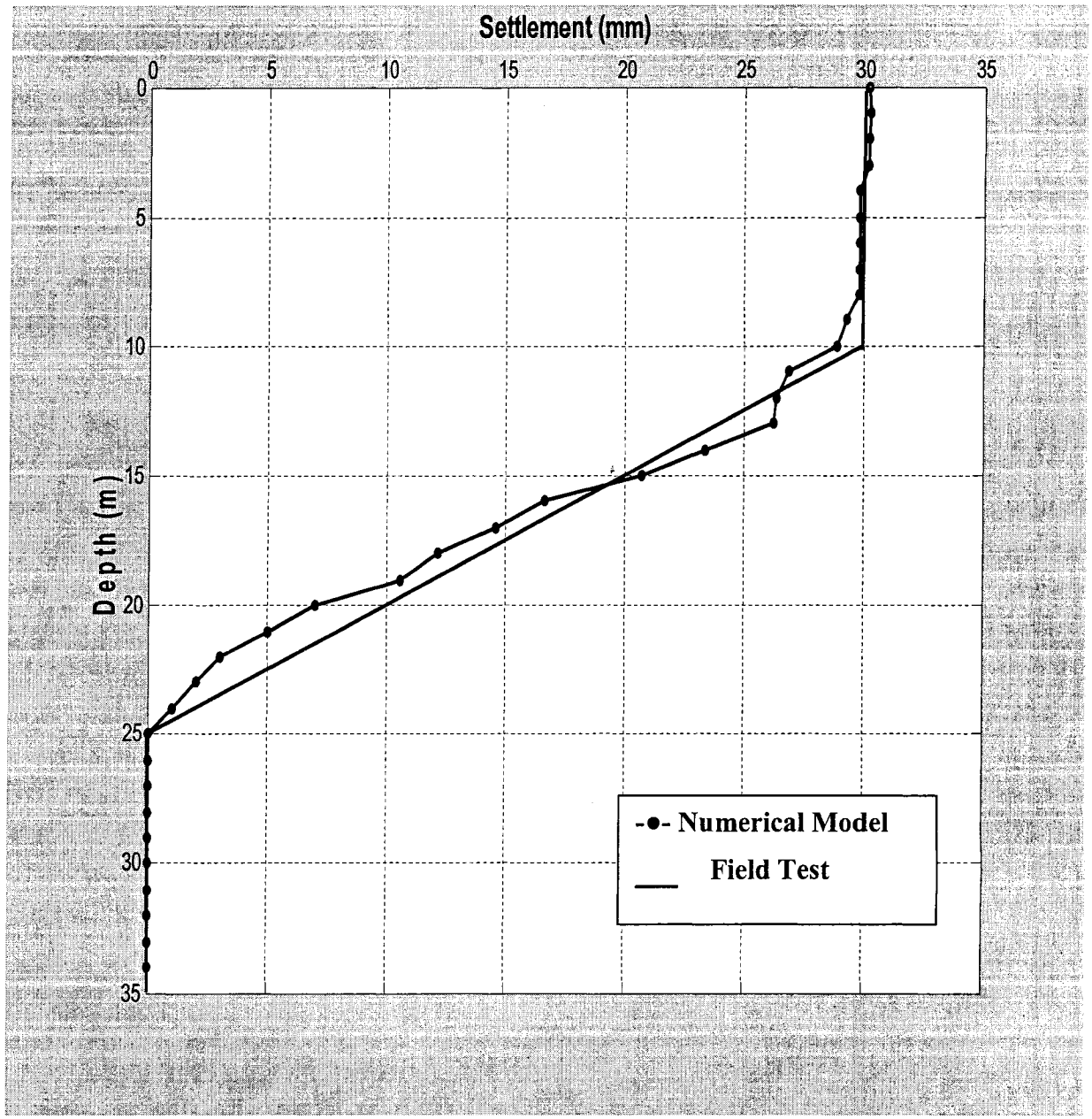

Fig. 3.11 Comparison between predicted and field measured values (Walker and Darvall, 1973) of the soil settlements.

CHAPTER 4

RESULTS AND ANALYSIS

4.1 General

After validating the numerical model developed in the present investigation, the numerical model was used then to produce results for a wide range of the parameters believed to govern the results. Time dependent skin friction along the pile shaft, settlement of soils, axial load distribution in the pile for variable thickness of soft clay layer has been presented herein. In addition, the location of the neutral plane with time and the effect of time on skin friction distribution are also presented in this chapter. Furthermore, the effect of the thickness of the soft clay layer on the distribution of the skin friction, settlement of soils and the location of neutral plane were examined.

4.2 Test Results

The present numerical model was used to develop data for a wide range of parameter, which believe to govern the behavior of skin friction. Tests were performed for different thickness ratio of soils, cohesion ratio, surcharge loads, and pile's length to diameter ratio. For each test, the skin friction distribution, axial loads, location of neutral plane, and dissipation of excess pore pressure with time are monitored for different ratio of the thickness.

Fig.4.1 presents the skin friction distribution of soft clay along the entire length of the pile versus time. It can be noted from this figure that the distribution of skin friction is changed with dissipation of excess pore water pressure. The final skin friction

distribution was achieved when pore water pressure reached a static level. In this figure the distribution of the skin friction was observed during both the undrained and drained periods until consolidation is completed. Fig. 4.2 presents the distribution of the excess pore water pressure with time. It is of interest to note that during these periods, the neutral plane change its location from 21.25 m to a depth 23.85 m from the pile cap. Fig.4.3 presents the settlement versus time curves for soft clay layer along the pile length. It can be noted that, when consolidation was completed, 198 mm settlement was recorded in soft clay layer.

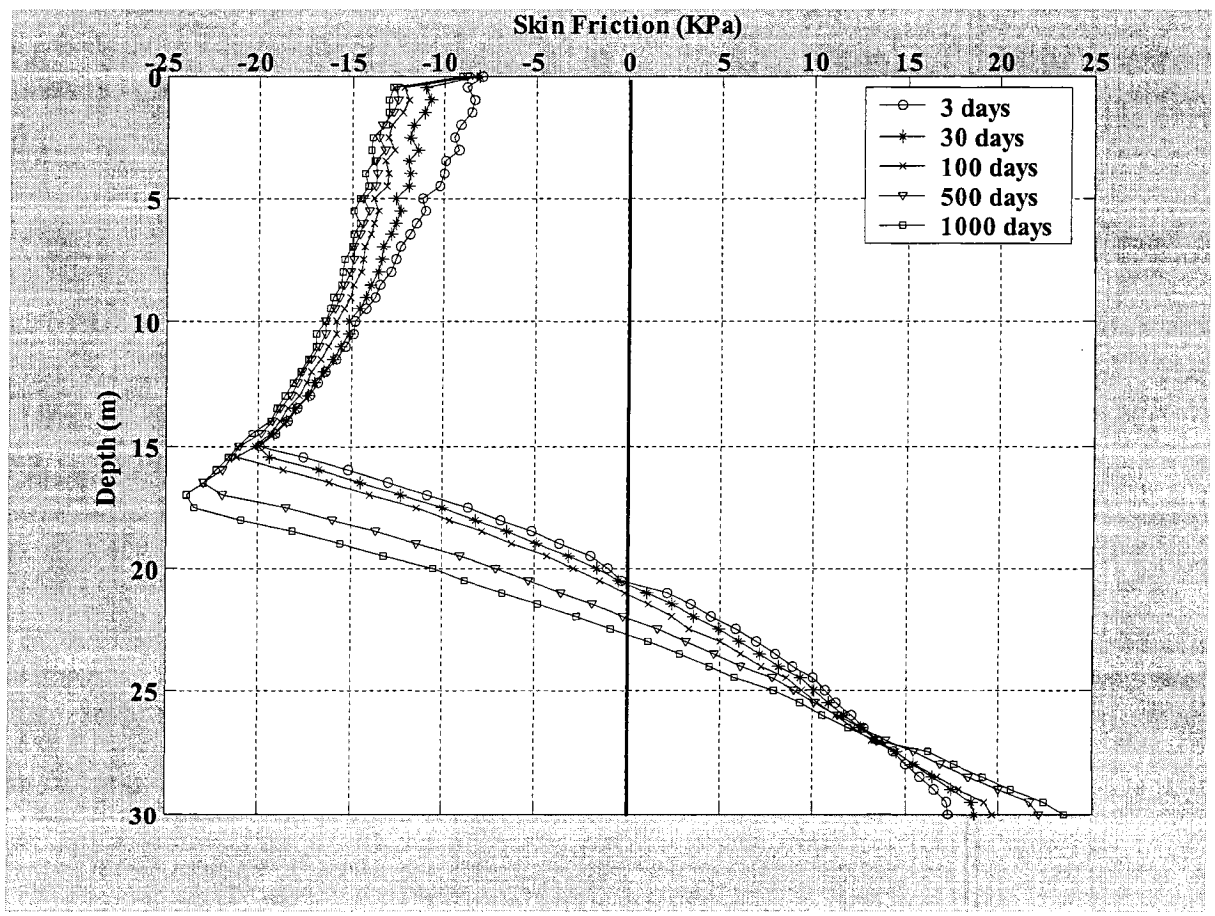

Fig. 4.1 Skin friction distribution for the soft clay layer along the pile length versus time (Surcharge loads = 60 kPa)

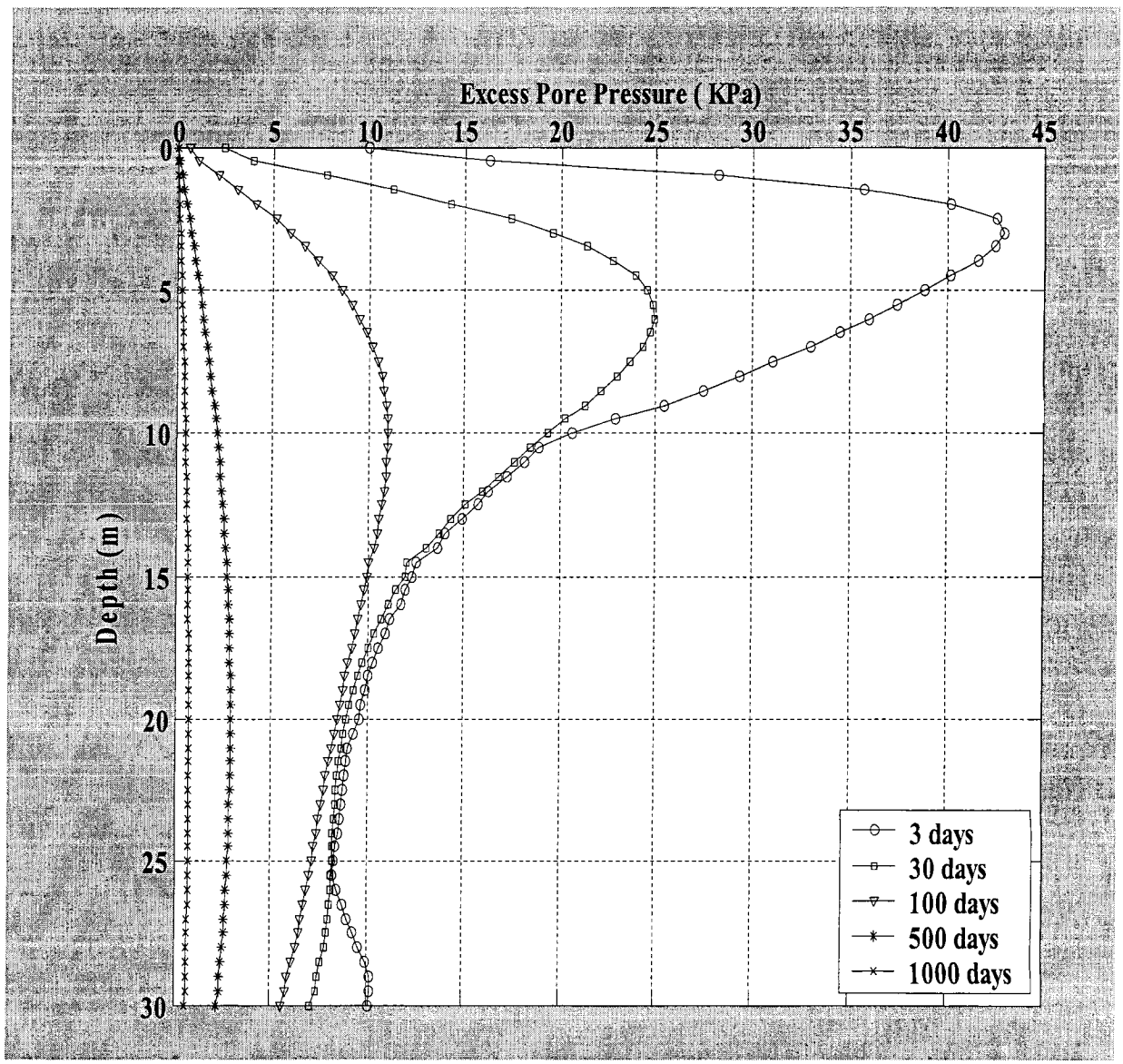

Fig. 4.2 Dissipation of excess pore pressure with time

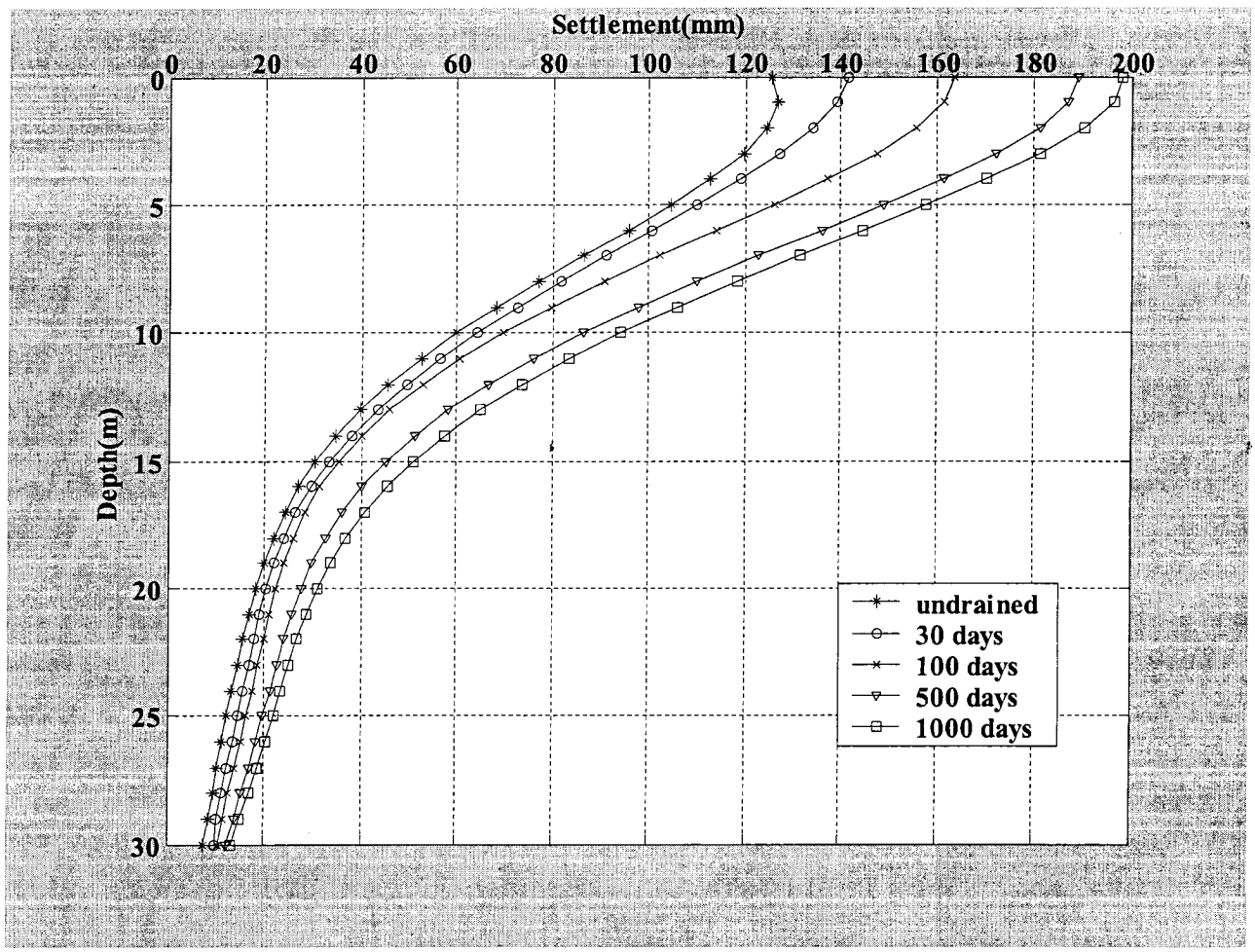

Fig. 4.3 Settlement of the soft clay layer along the pile length versus time (Surcharge loads = 60 kPa)

Fig. 4.4 presents the short and the long term skin friction distribution for the thickness ratio of 0.8. It can be noted from this figure that the neutral plane changed its location from 21.18 m to 23.20 m from pile cap during consolidation. The long term settlement of clays was found 195 mm. The settlement curves of the short and long term for this thickness ratio is shown in Fig. 4.5.

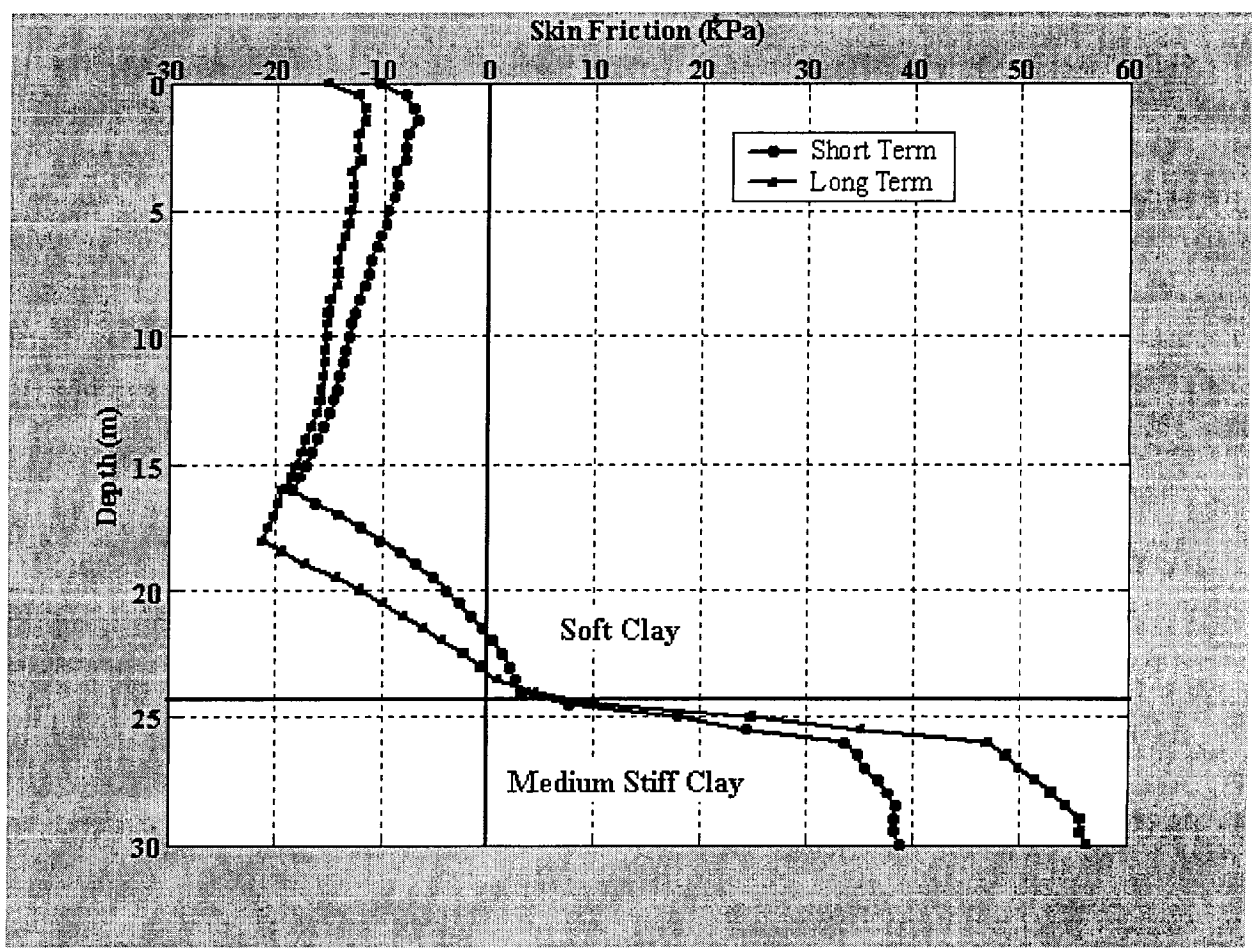

Fig. 4.4 Short and long term skin friction distribution (Thickness ratio = 0.8, Cohesion ratio = 0.2, Surcharge loads = 60 kPa)

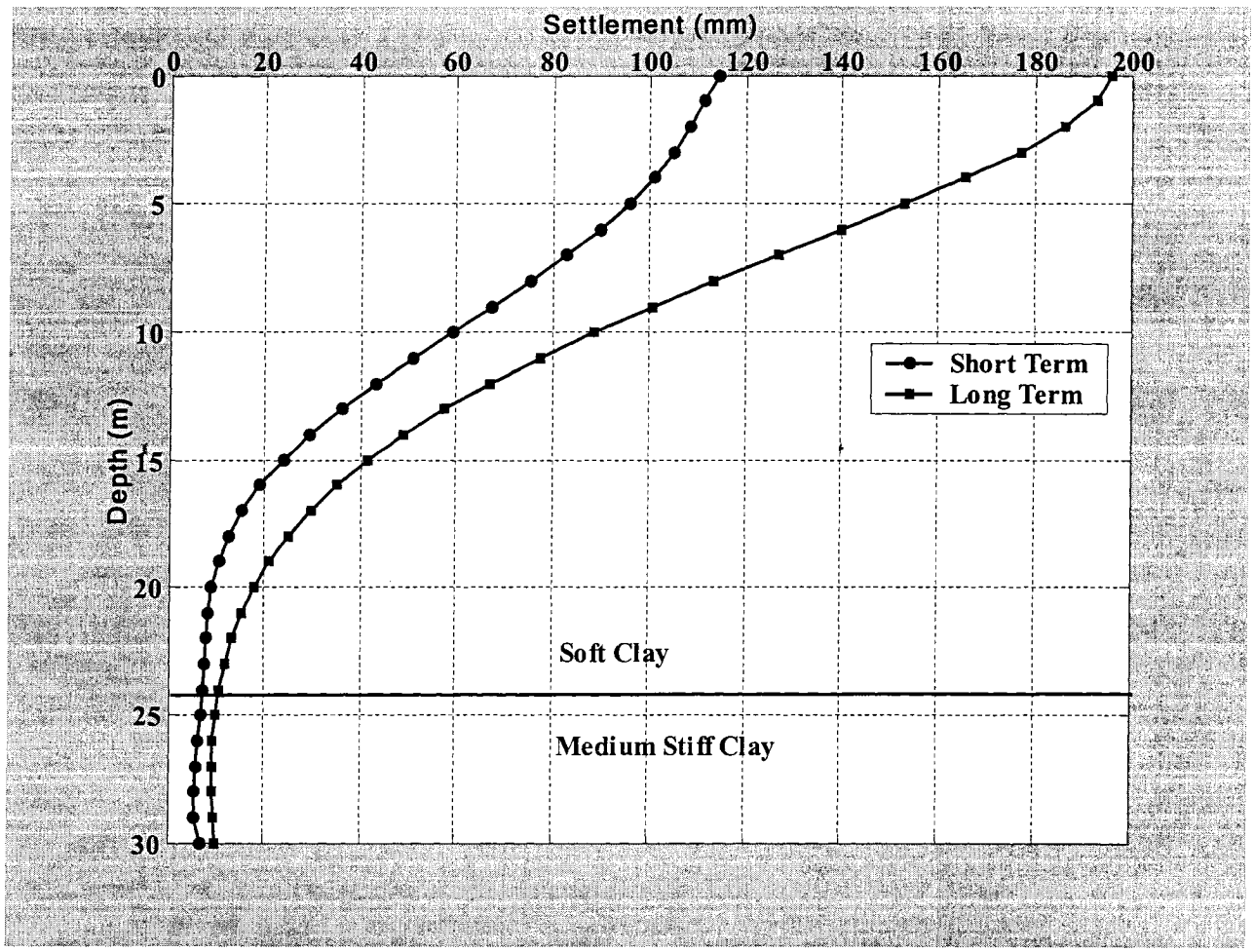

Fig. 4.5 Short and Long term settlement curves (Thickness ratio = 0.8, Cohesion ratio = 0.2, Surcharge ratio = 60 kPa)

It is of interest to note that although a good agreement between short and long term can be found for the thickness ratio of 0.6, the location of neutral plane remained nearly unchanged during consolidation (Fig.4.6), while the soft clay layer settled about 177 mm during consolidation, as shown in Fig. 4.7.

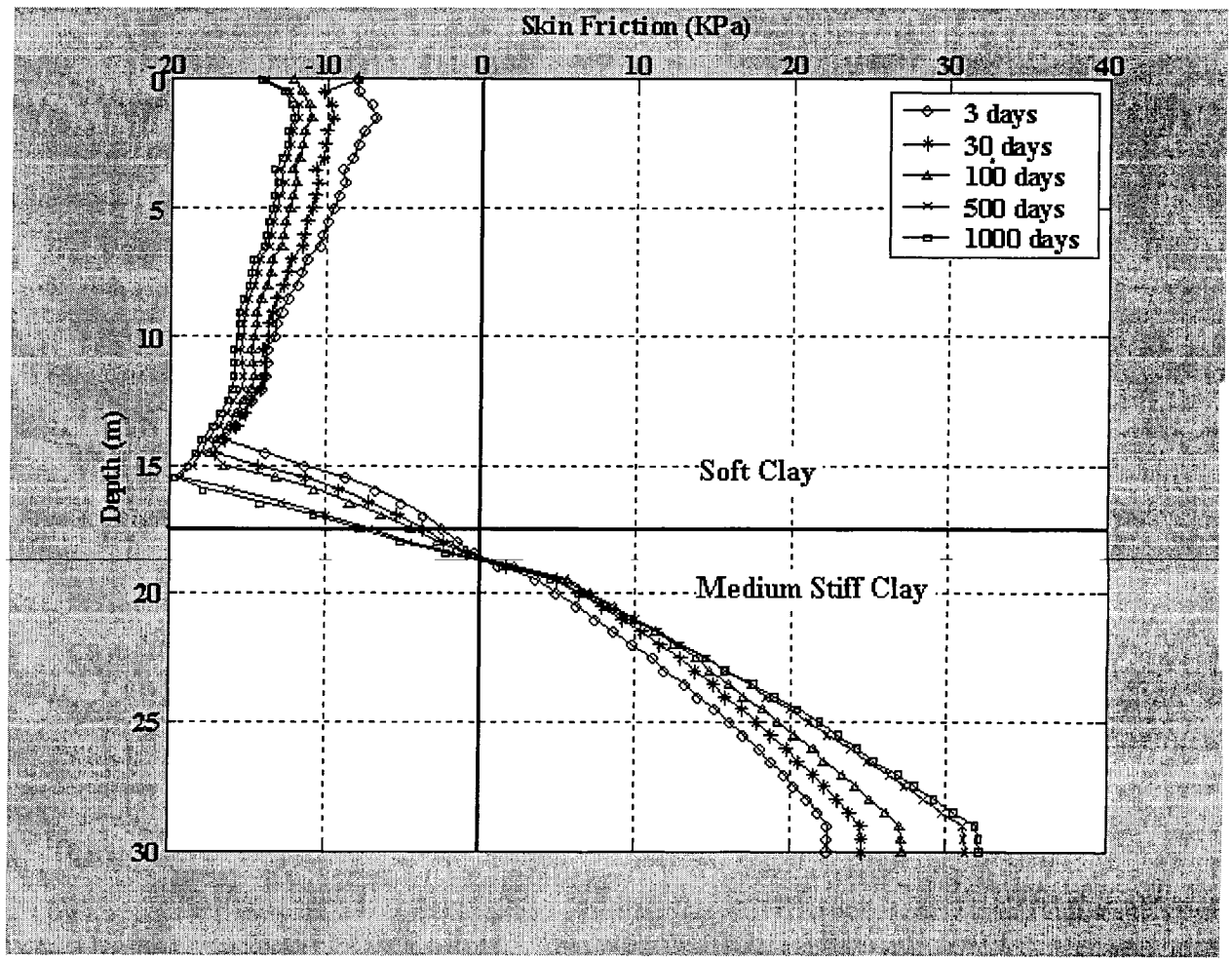

Fig. 4.6 Time dependent skin friction distribution (Thickness ratio = 0.6, Cohesion ratio = 0.2, Surcharge loads = 60 kPa)

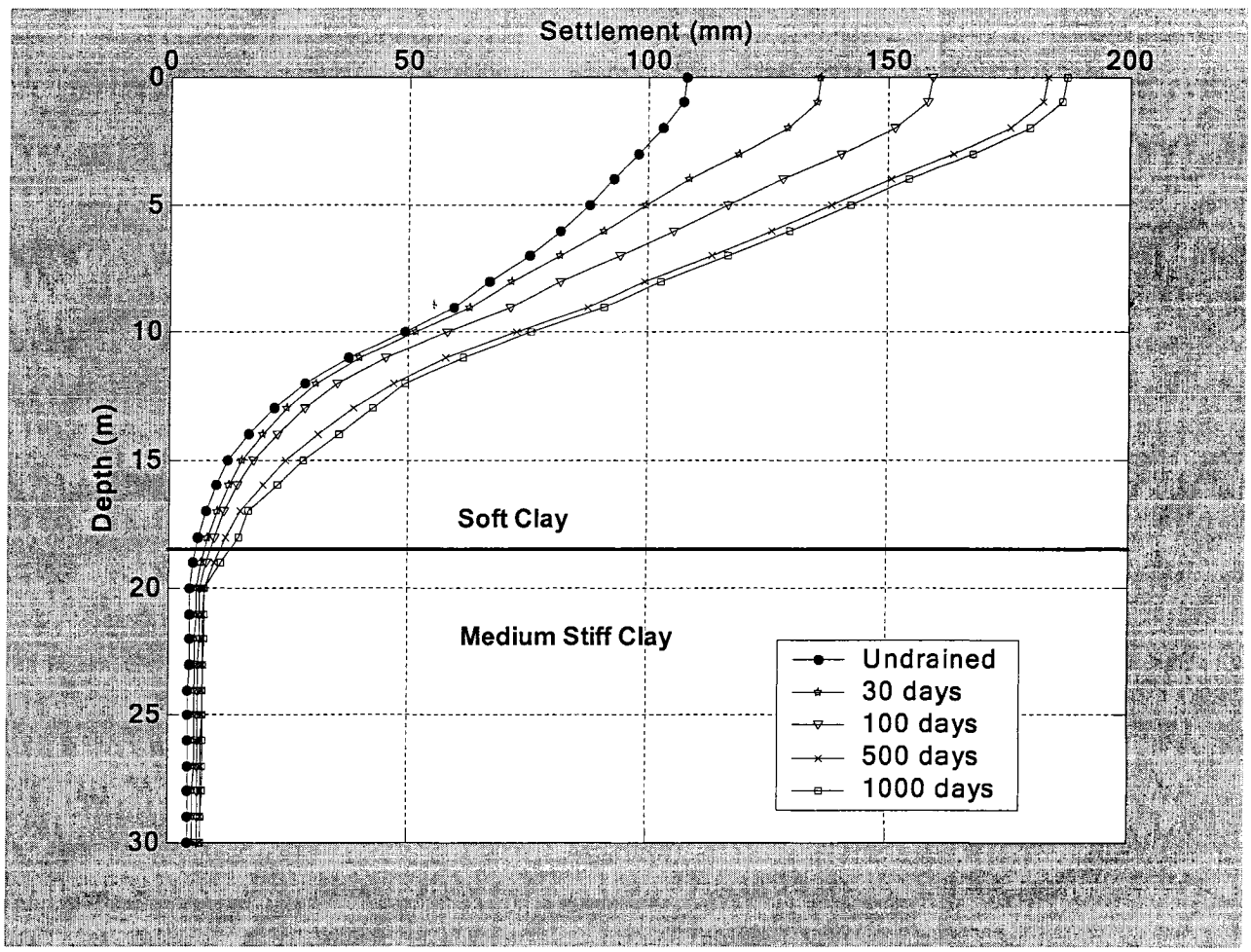

Fig. 4.7 Time dependent settlement of soft clay (Thickness ratio = 0.6, Cohesion ratio = 0.2, Surcharge loads = 60 kPa)

Fig.4.8 presents the maximum axial loads found at the location of neutral plane during the undrained period and after the consolidation was completed were 280 kN and 430 kN respectively.

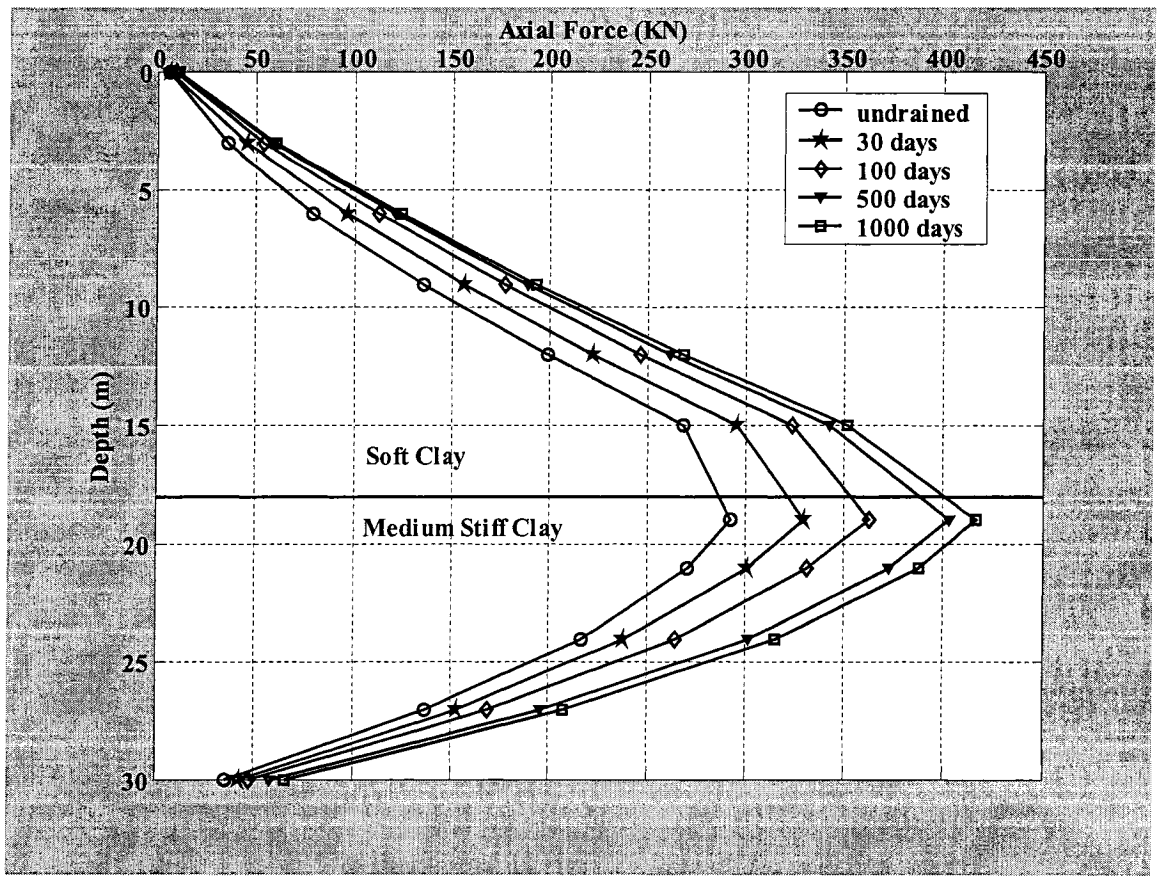

Fig. 4.8 Axial loads on pile with time (Thickness ratio = 0.6, Cohesion ratio = 0.2, Surcharge loads = 60 kPa)

Time dependent skin friction distribution for thickness ratio 0.5 is shown in Figs. 4.9. In this test, the neutral plane was found at a depth 18.35m during undrained period. When consolidation was completed, the neutral plane was found at a depth 18.70m from the pile cap. Settlement of soft clay with time was observed and shown in Fig. 4.10.

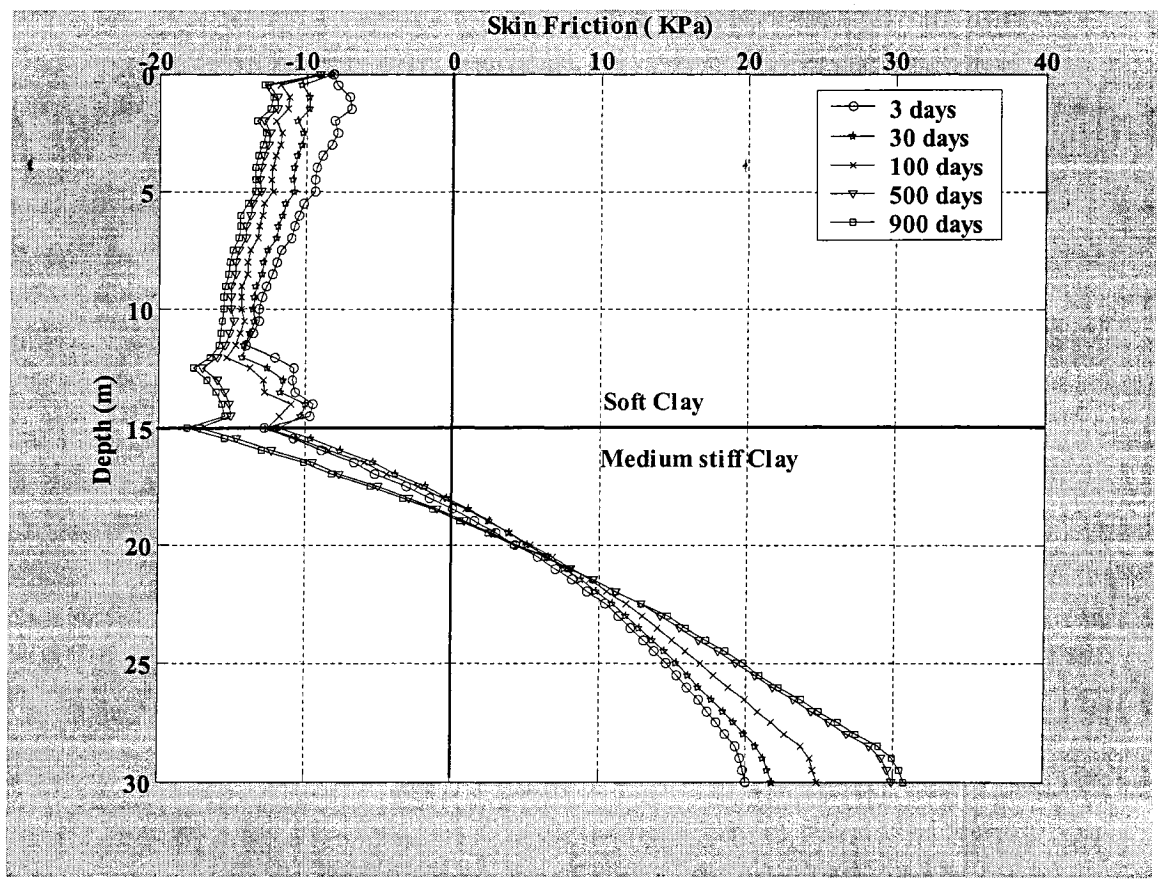

Fig. 4.9 Time dependent skin friction distribution (Thickness ratio = 0.5, Cohesion ratio = 0.2, Surcharge loads = 60 kPa)

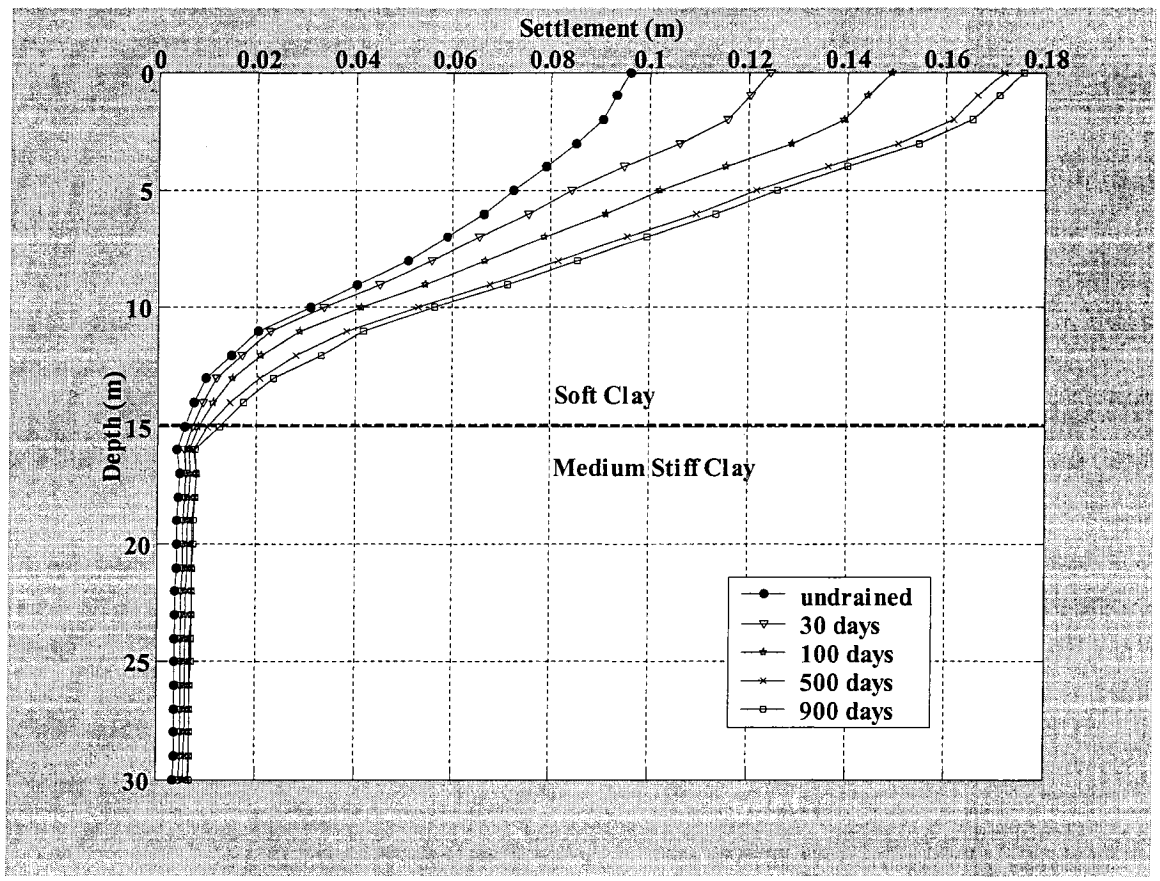

Fig. 4.10 Time dependent settlement of clay (Thickness ratio = 0.5, Cohesion ratio =0.2, Surcharge loads = 60 kPa)

For thickness ratio 0.3, time dependent skin friction distribution is shown in Fig. 4.11. It can be noted from this figure that the neutral plane changed its location from 16.83m to a depth of 17.48m from undrained period to completion of consolidation as found in stiff clay. Settlement of soft clay with time is shown in Fig.4.12.

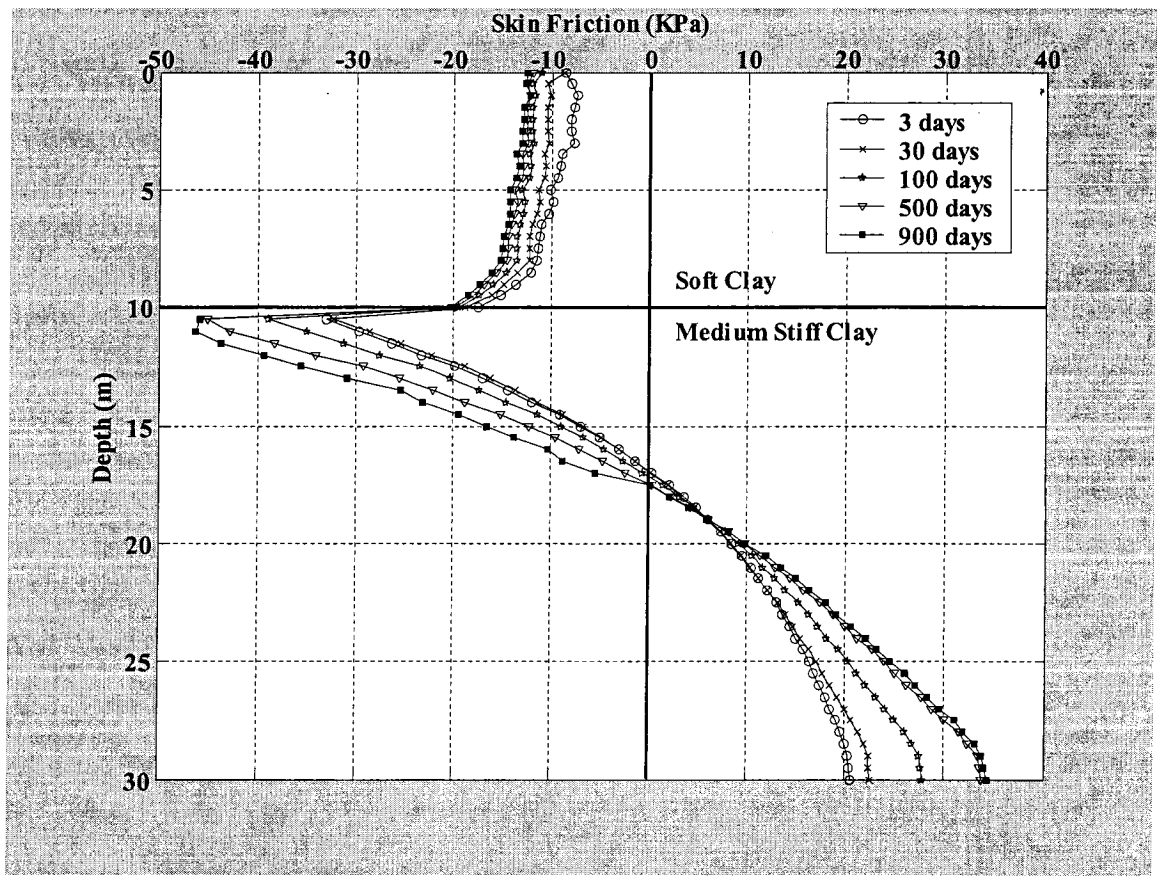

Fig. 4.11 Skin fiction distribution versus time (Thickness ratio = 0.3, Cohesion ratio 0.2, Surcharge loads = 60 kPa)

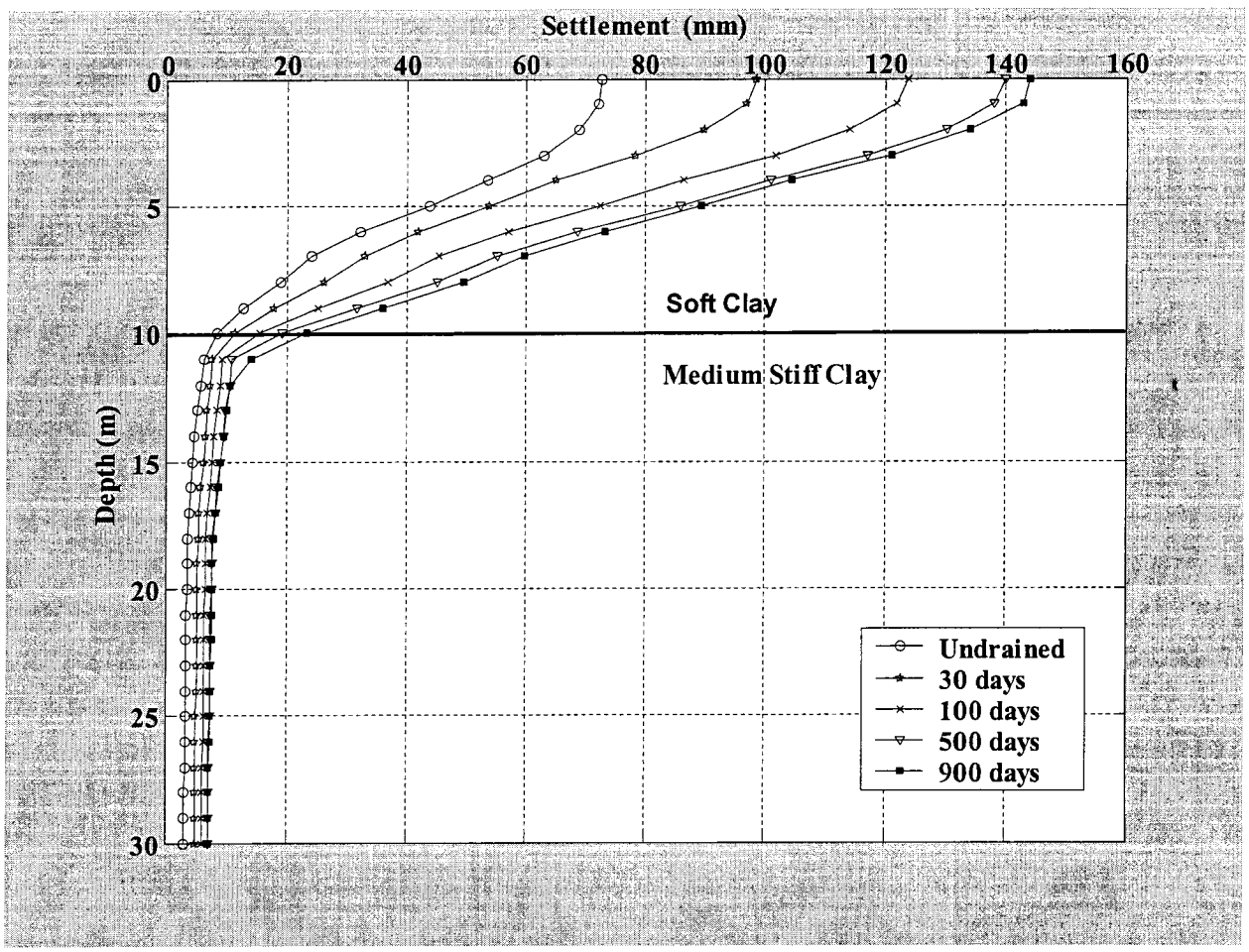

Fig. 4.12 Settlement of clay versus time (Thickness ratio = 0.3, Cohesion ratio = 0.2, Surcharge loads = 60 kPa)

Figs. 4.13 to 4.17 present the short and the long term skin friction distributions for thickness ratios 0.15, 0.25, 0.40, 0.55, and 0.70 respectively.

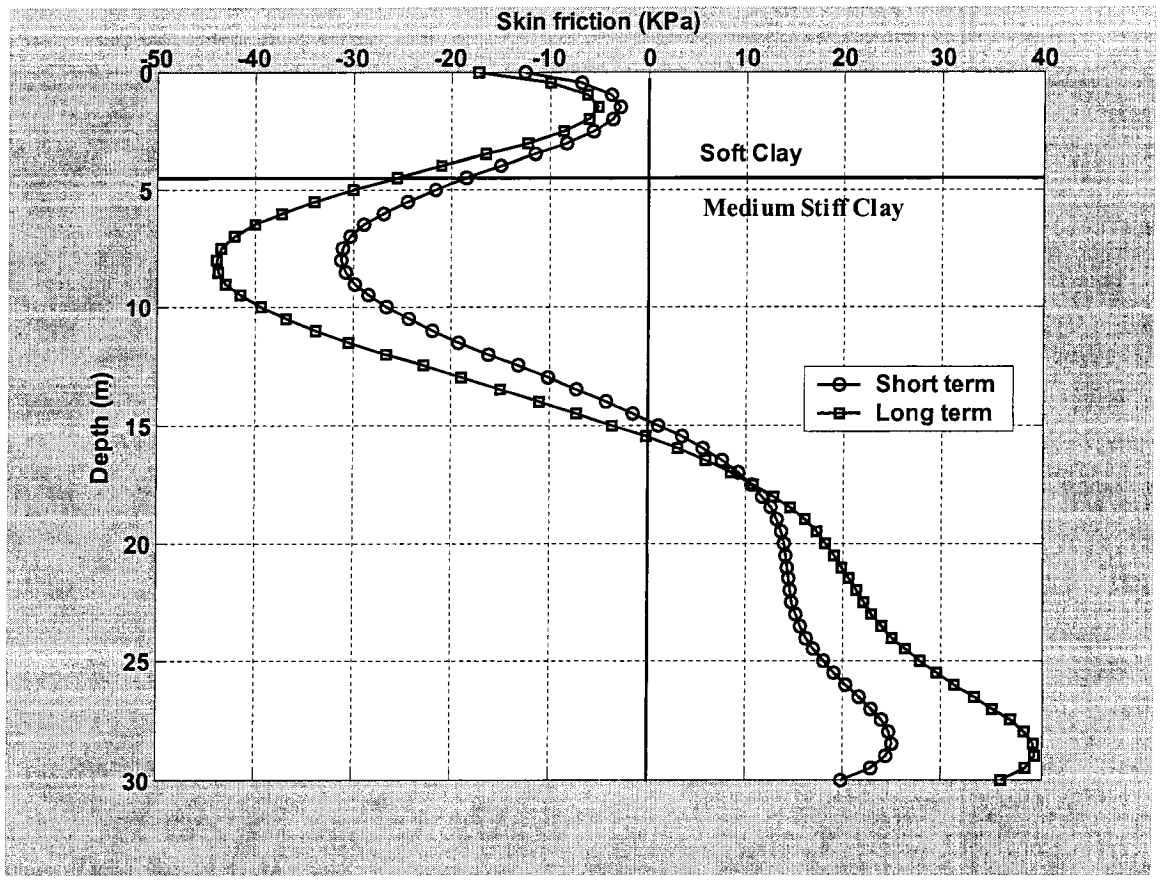

Fig. 4.13 Short and long term skin friction distributions (Thickness ratio = 0.15, Cohesion ratio =0.2, Surcharge loads=60 kPa)

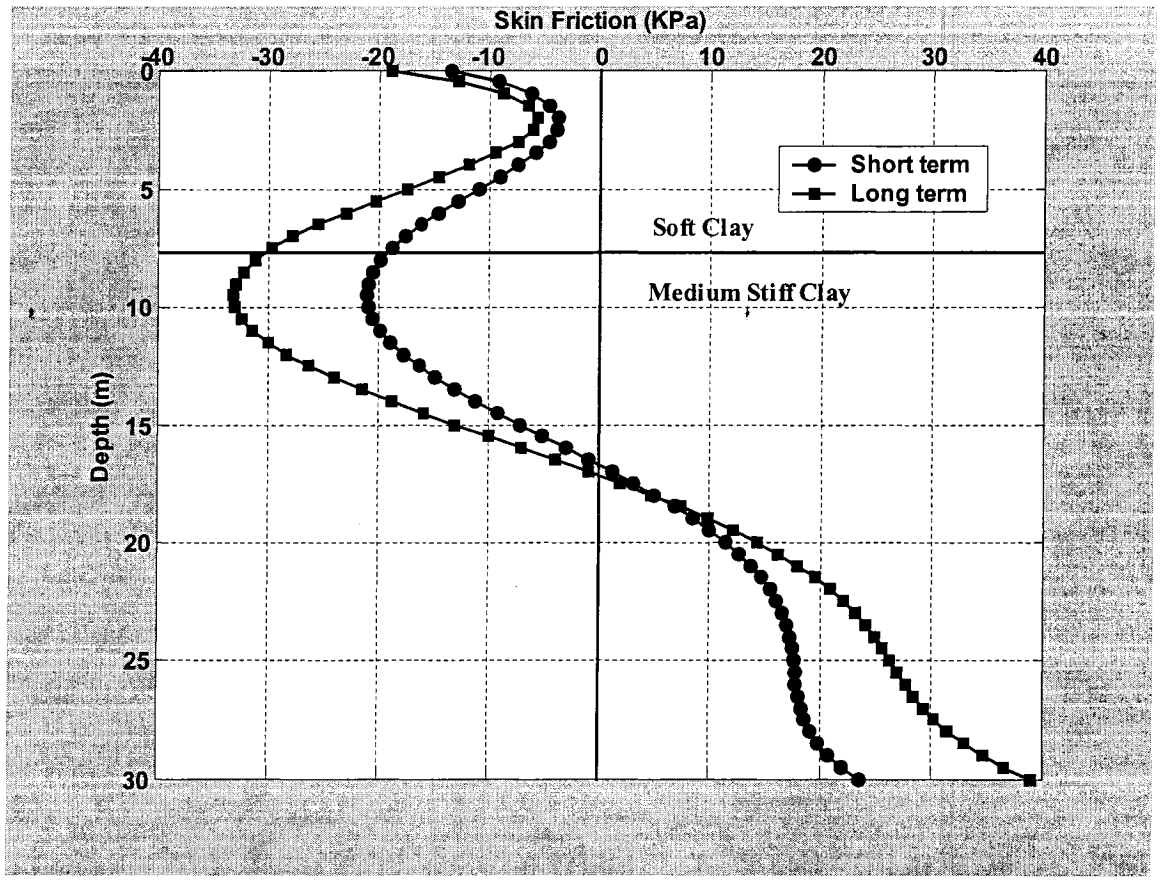

Fig. 4.14 Short and long term skin friction distributions (Thickness ratio = 0.25, Cohesion ratio =0.2, Surcharge loads = 60 kPa)

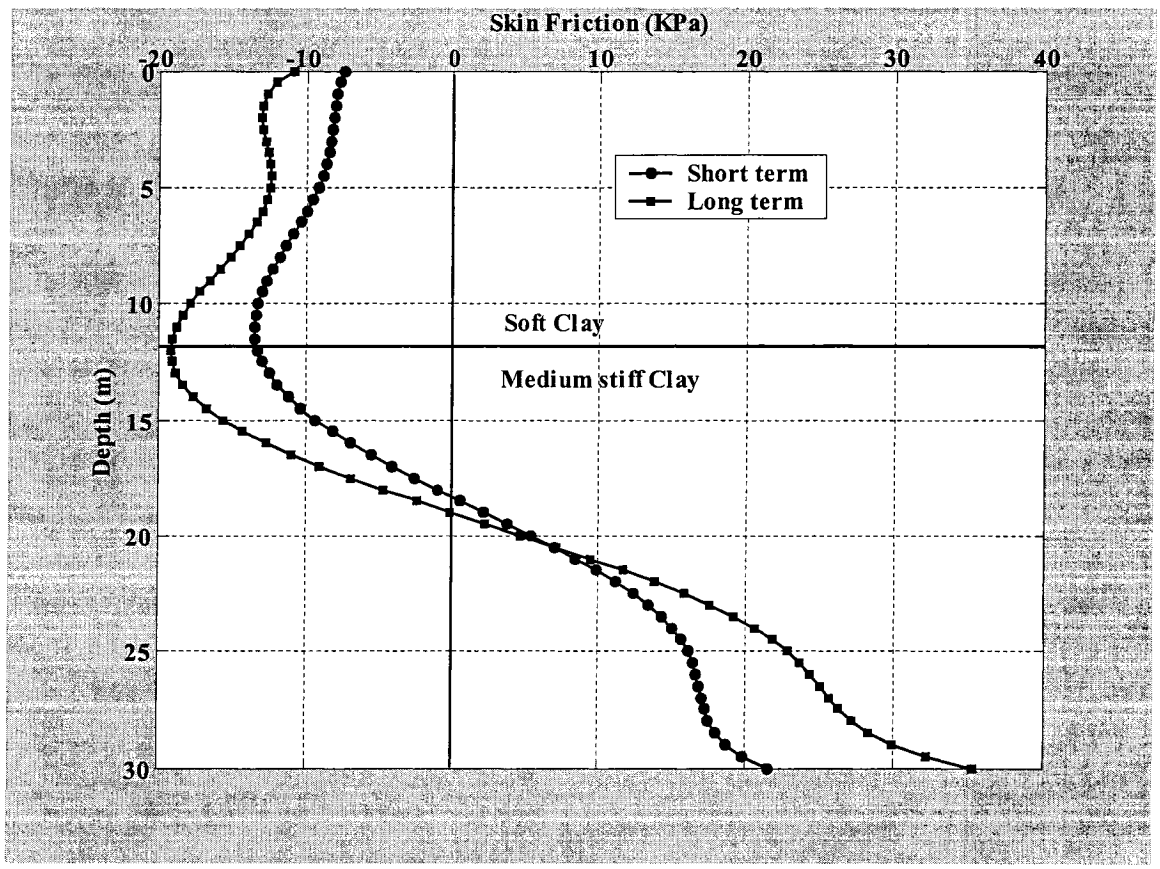

Fig. 4.15 Short and long term skin friction distributions (Thickness ratio = 0.40, Cohesion ratio = 0.2, Surcharge loads =60 kPa)

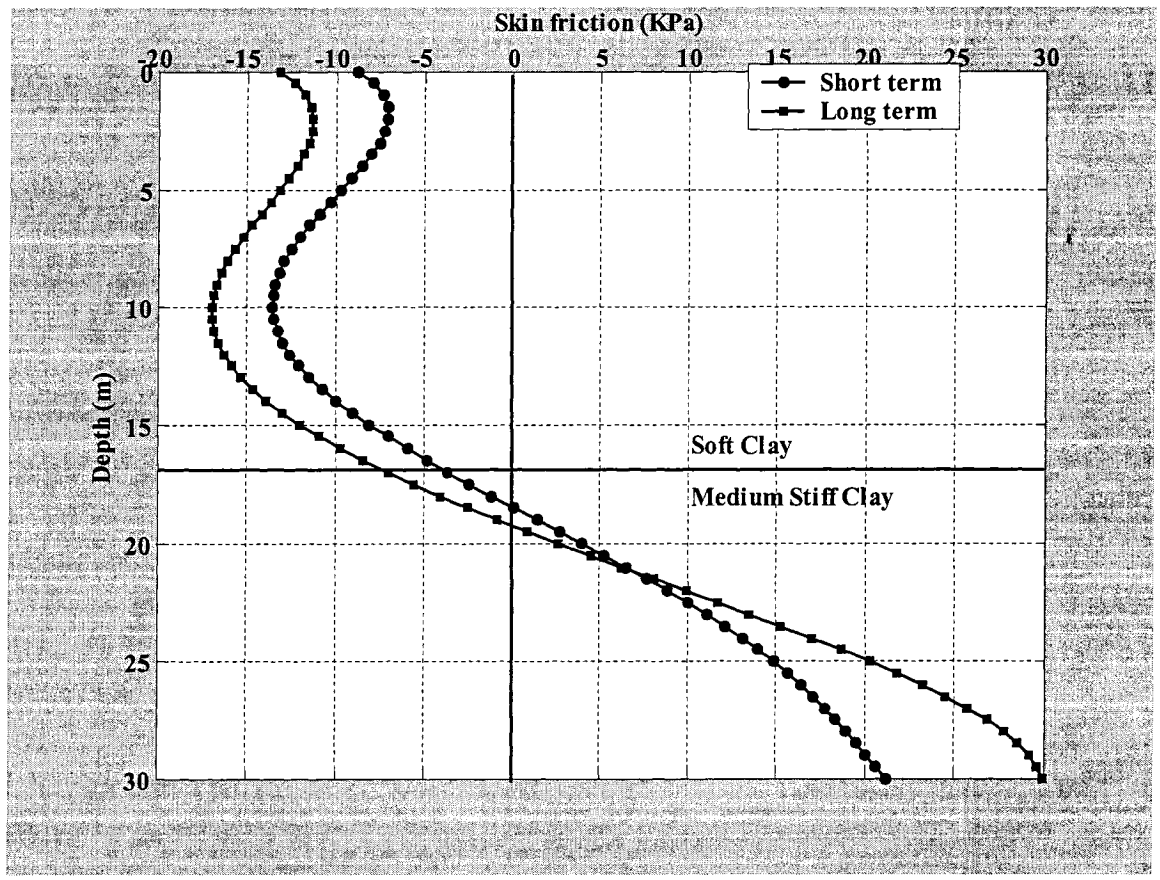

Fig. 4.16 The short and long term skin friction distributions (Thickness ratio = 0.55, Cohesion ratio =0.2, Surcharge loads= 60 kPa)

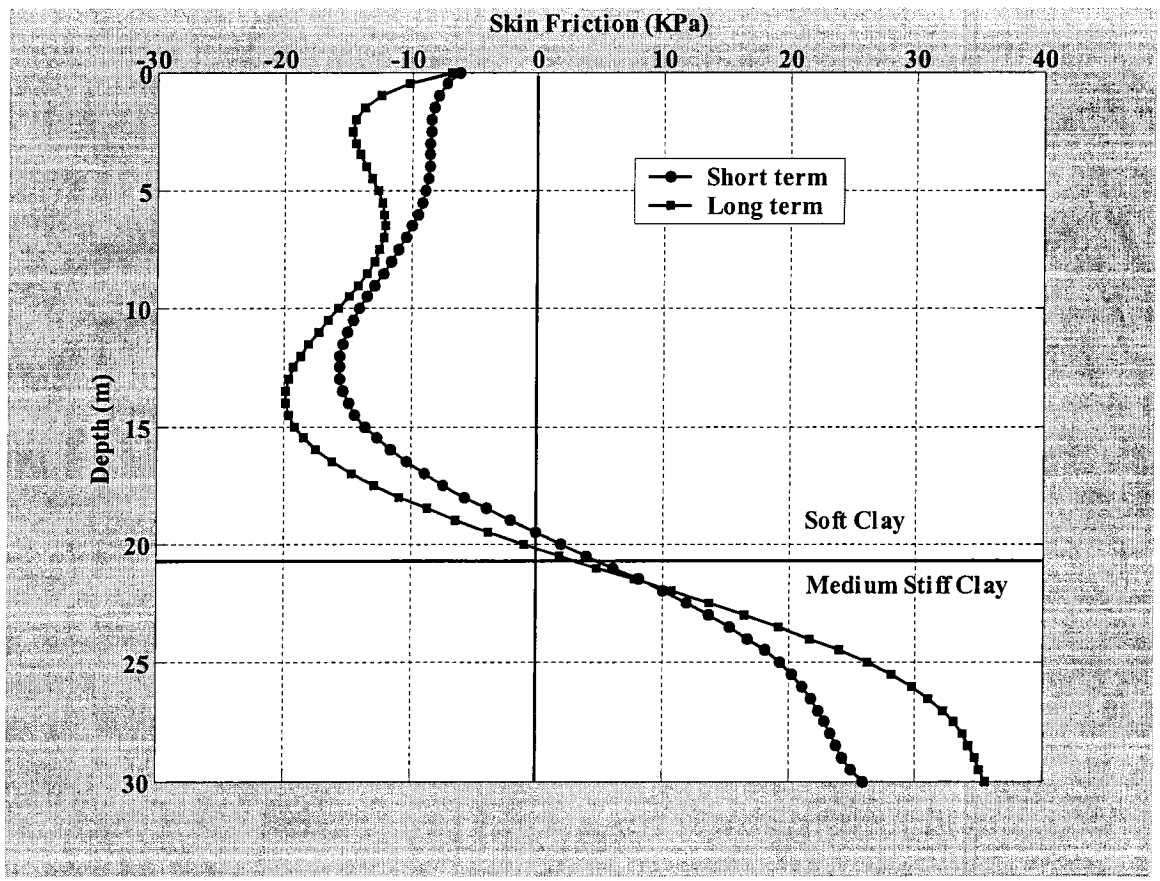

Fig. 4.17 Short and long term skin friction distributions (Thickness ratio = 0.70, Cohesion ratio = 0.2, Surcharge loads = 60 kPa)

4.3 Sensitivity Analysis

In this study, the parameter that governs the skin friction distribution, namely: the axial loads, position of neutral plane, and the bearing capacity of pile, and the thickness ratio of soft clay embedded along the pile surface. It is found that the magnitude of negative skin friction differ with the variation of soft clay thickness ratio. During the consolidation process, the excess pore pressure dissipates and the skin friction curves become wider until total dissipation of excess pore pressure. Consequently, wide skin friction curves were observed during the drained period than for the undrained period. A greater magnitude of skin friction contributes higher amount of axial loads on piles and the maximum amount of axial loads is obviously found at the neutral plane location. From the present study, it is also found that piles may experience downdrag loads depending on the magnitude of surcharge loads without the presence of soft clay layer (Fig. 4.18).

Neutral plane is found at different locations for different ratios of clay thickness along the pile length. In general, neutral plane changes location during consolidation period. However, during consolidation neutral plane may not change its location, or a minor change occurs in neutral plane location for smaller thickness ratio. Location of neutral plane is essential for determining the amount of downdrag loads caused due to surcharge loads. Piles may experience higher amount of downdrag loads for smaller thickness ratio if the neutral plane is found at a significant depth in stiff clay. In fact, the location of neutral plane depends on the amount of surcharge loads, cohesion ratio of soft to stiff clay, and the thickness ratio of clays. Time dependent change in neutral plane location with variation of thickness ratio is shown in Table 4.1. A wide change in neutral plane location is occurred from short to long term with a higher thickness ratio then it

increases in smaller amount with a decrease in thickness ratio. Change in neutral plane location versus thickness ratio is shown in Fig. 4.19. Nevertheless, location of neutral plane does not change, or change a minor amount for different pile length to diameter ratio as shown in Fig. 4.20.

In addition, the downdrag loads on pile do not differ significantly for a small increase or decrease of thickness ratio. However, greater difference in magnitude of downdrag loads is found for large variation in thickness ratio. Sometimes, large magnitude of downdrag loads is found on piles for a small thickness ratio. This may happen due to large surcharge loads that caused excessive settlement of underneath soil.

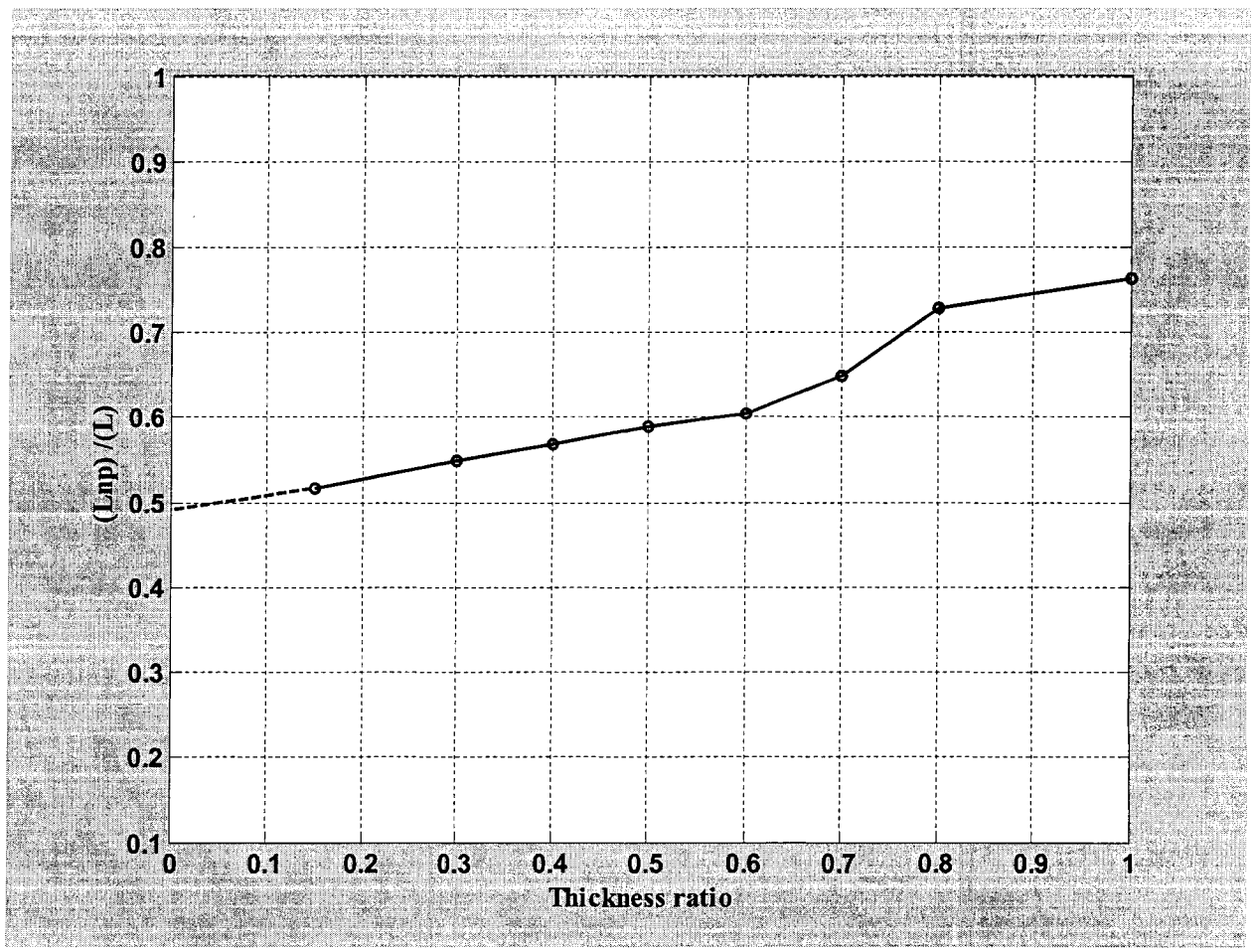

Fig. 4.18 Location of neutral plane versus the thickness ratio (Cohesion ratio = 0.4, Surcharge loads = 60 kPa)

Thickness ratio	Short term location of Neutral Plane (m)	Long term Location of Neutral Plane (m)	Change in Neutral Plane Location (m)
1	21.25	23.85	2.60
0.8	21.18	23.20	2.02
0.7	19.91	20.62	0.70
0.6	18.81	18.91	0.10
0.55	18.63	18.78	0.15
0.5	18.35	18.70	0.35
0.4	17.65	18.05	0.40
0.3	16.83	17.48	0.62
0.25	16.30	16.96	0.66
0.15	15.90	16.61	0.71

Table 4.1 Short and long term location of neutral plane for different thickness ratio

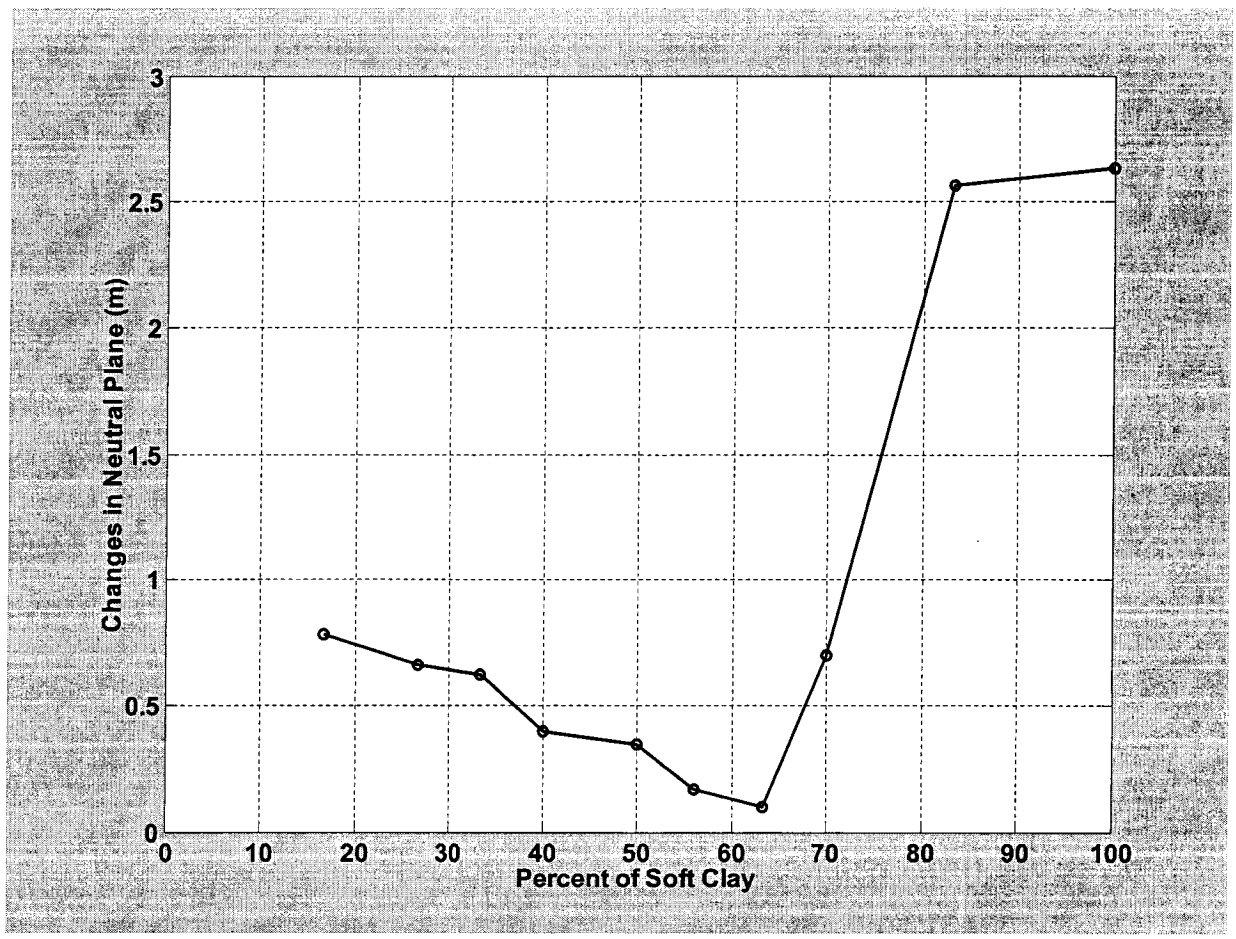

Fig. 4.19 Change in neutral plane location versus the thickness ratio

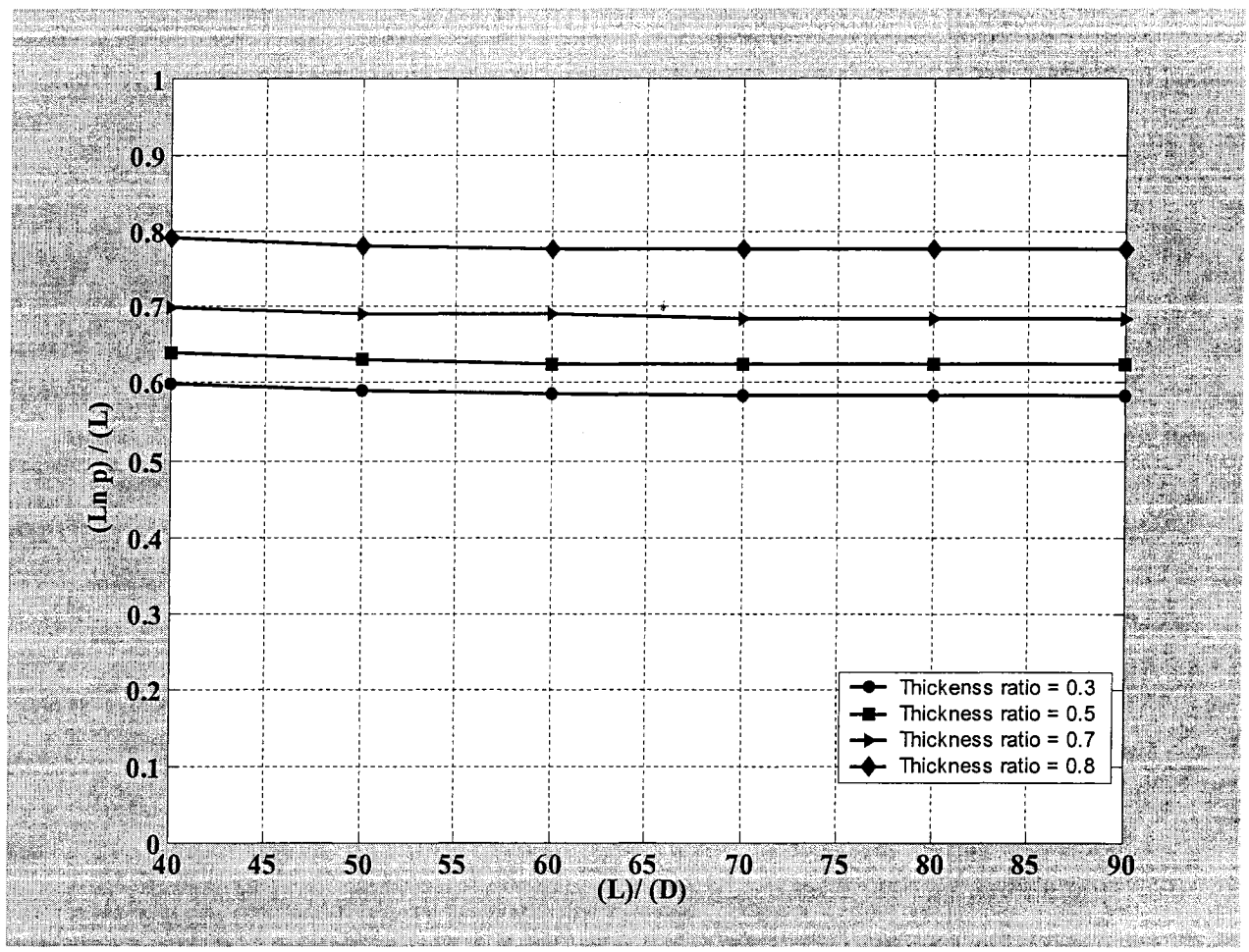

Fig. 4.20 Location of the neutral plane versus pile length to diameter ratio

4. 4 Discussion

The distribution of the skin friction along the pile's shaft was examined for piles in layered clay soils subjected to axial and surcharge loadings. The distribution was determined for different thickness ratio, cohesion ratio, and surcharge loads. In addition, the skin friction distribution was determined for both undrained and drained periods. It was established in this analysis that the location of the neutral plane is time dependent and varies significantly with the thickness ratio of the soils. A significant change in neutral plane location occurred during the drained period for higher thickness ratio as compared for lower thickness ratio.

Almost a linear variation in neutral plane location was found for different cohesion ratio of soils with equal magnitude of surcharge loads. Neutral plane location does not change for different pile length to diameter ratio for same soil parameters and loading condition. Therefore, the parameters that govern the position of neutral plane are cohesion ratio, thickness ratio of soil and surcharge loads. After detaining the location of the neutral plane, the zone for bitumen coating can be established to significantly reduce the negative skin friction and accordingly to enhance the capacity of pile.

4.5 Design Loads

In general, piles are settled due to two types of loads.

1. Applied loads
2. Downdrag loads

Applied loads cause settlements of piles in addition to the settlements due to downdrag loads from negative skin friction. This excess settlements of piles due to applied loads results in shifting the location of neutral plane from its position due to surcharge loads. The distance of neutral plane ***Lnp*** will be reduced due to applied loads. Consequently, downdrag loads will be reduced due to reduction of neutral plane distance from pile head. When total settlement of piles due to applied loads and downdrag loads is higher than the settlements of adjacent soil, downdrag loads need not to be included in calculating bearing capacity of pile. However, downdrag loads need to be included in calculating bearing capacity of pile if adjacent soil's settlement is higher than the pile settlement due to applied loads and downdrag loads. From the present study, it is seen that neutral plane location is shifted from 50 percent to 75 percent of pile length approximately for different thickness ratio. In practical, this location of neutral plane will be shifted in upward direction due to applied loads. It is difficult to determine the exact movement of neutral plane in upward direction since applied loads is unpredictable. Therefore, a reduction factor, $\boldsymbol{R_f}$ is incorporated in order to determine the final location of neutral plane. $\boldsymbol{R_f}$ is assumed to be varied from 0.1 to 0.2.

4.6 Design Charts

Based on thickness ratio, cohesion ratio, and the magnitude of surcharge loads, design charts are developed to determine the location of neutral plane. Distance of neutral plane from pile head will be used in order to calculate downdrag loads. Design charts are shown from Fig. 4.21 through Fig. 4.23.

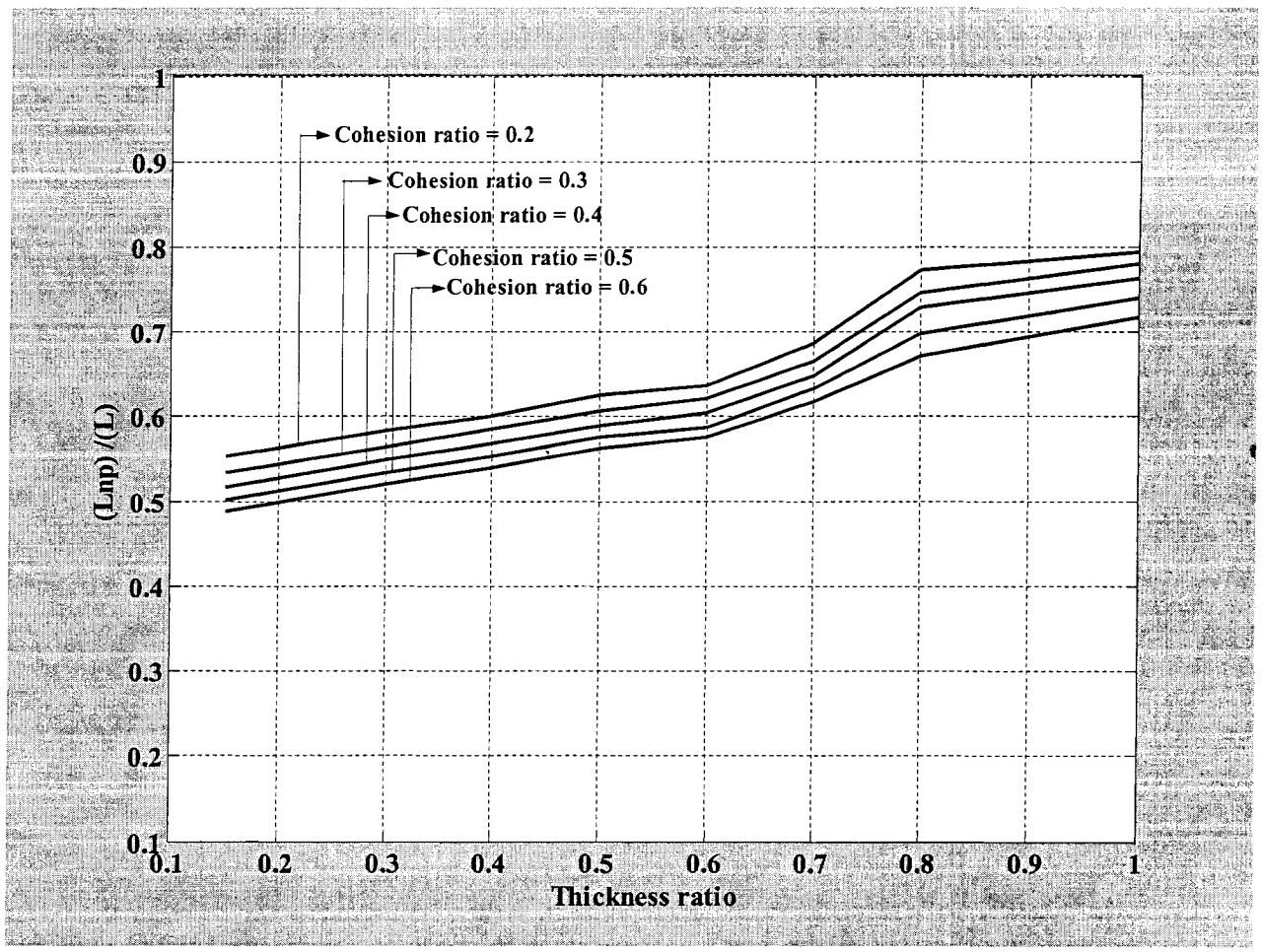

Fig.4.21 Design Chart -Depth of neutral plane as a function of thickness ratio and cohesion ratio (Surcharge loads = 60 kPa)

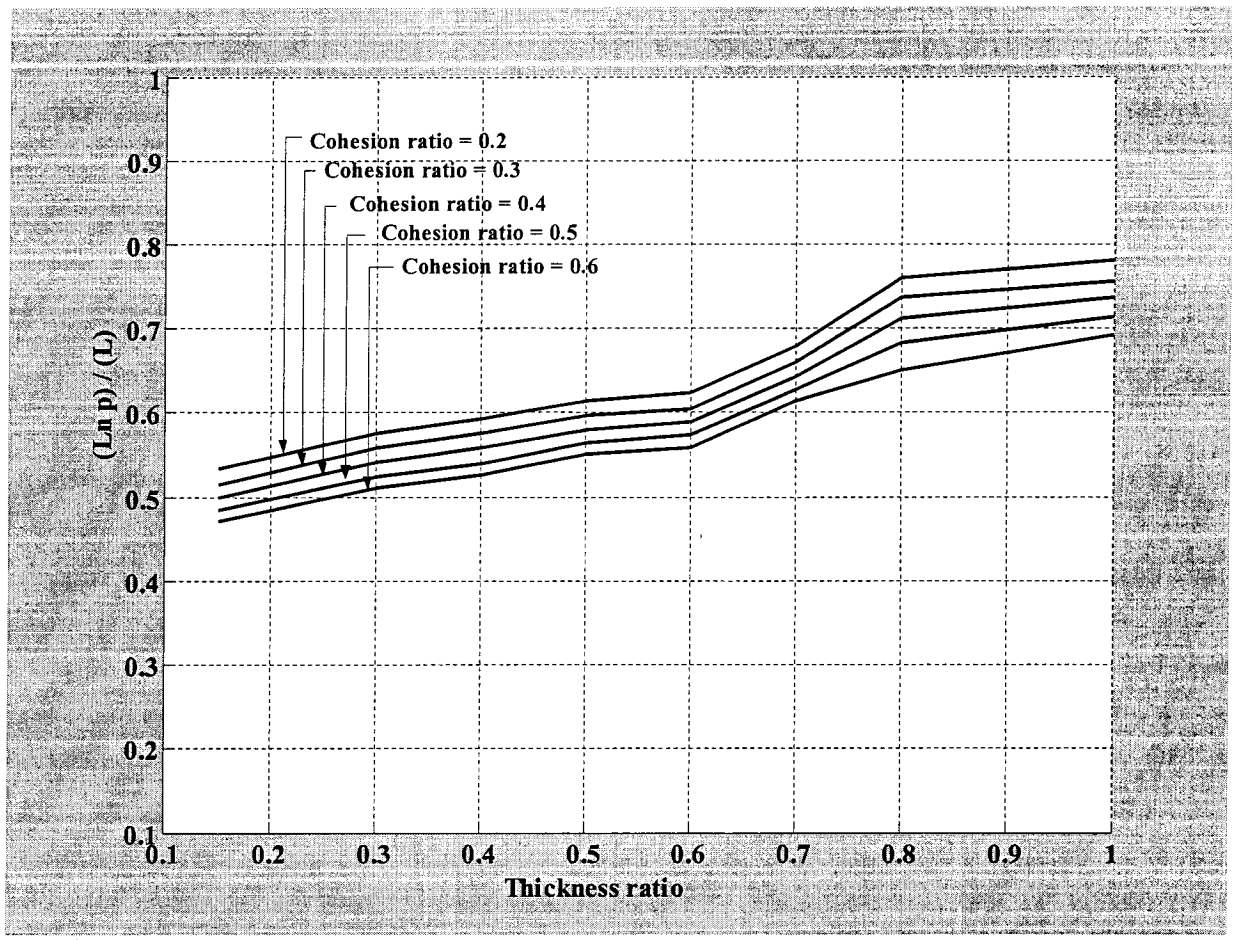

Fig.4.22 Design Chart -Depth of neutral plane as a function of thickness ratio and cohesion ratio (Surcharge loads = 50 kPa)

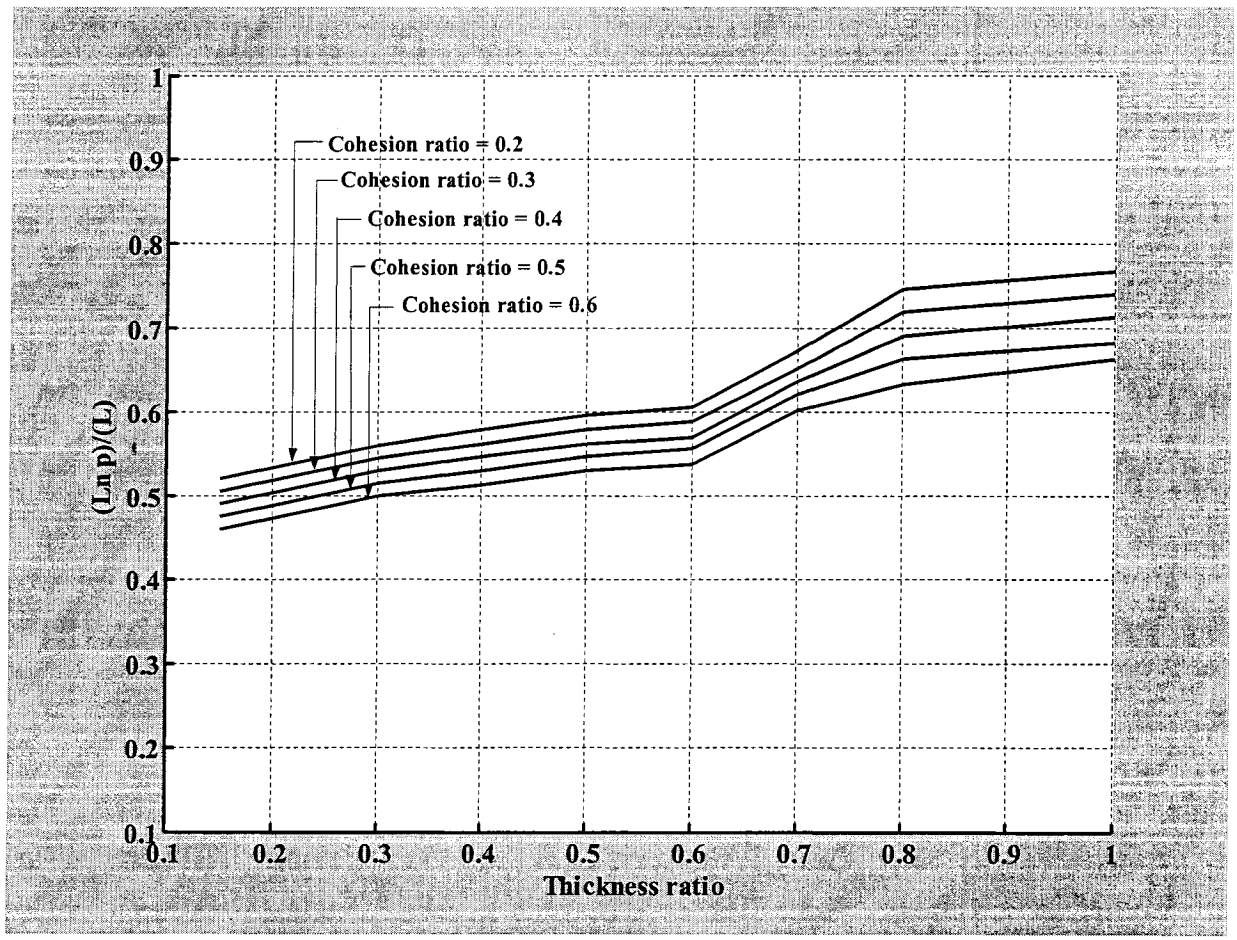

Fig.4.23 Design Chart - Depth of neutral plane as a function of thickness ratio and cohesion ratio (Surcharge loads = 40 kPa)

4.7 Design Procedure

The following formula for calculating skin friction had been proposed by Johannessen and Bjerrum (1965).

$$\mathbf{F}s = \sigma_v^{'} K \tan\delta$$

$$= \beta\sigma_v^{'} \quad \text{.....} \quad \textbf{(4.1)}$$

Where,

Fs = skin friction per unit area

$\sigma_v^{'}$ = effective vertical stresses in soil

K = Coefficient of earth pressure

δ = Angle of friction between soil and pile

β = K$\tan\delta$

Based on the above formula downdrag loads at a depth z can be expressed as

$$\mathbf{Q} = \int_0^z (\beta\sigma_v^{'})(\pi d)dz$$

$$= \int_0^z \beta(\gamma' z + S)(\pi d)dz \quad \text{.....} \quad \textbf{(4.2)}$$

Where,

Q = downdrag loads at depth z

d = diameter of pile

γ'= effective unit weight of soil

S = Surcharge loads

Considering a single pile of 30 m in length and 500 mm in diameter embedded in 20 m soft clay overlaid a layer of stiff clay of 15 m thickness. Soft clay layer is subjected to

surcharge loads of 50 kPa. The cohesion of soft and stiff clay is 10 kPa and 50 kPa respectively. Effective unit of soft and stiff clay is found 7.0 kN/m^3 and 9.2 kN/m^3 respectively. β is taken 0.25 with a factor of safety is 2.

The downdarg force, shaft resistance, and tip resistance must be calculated in order determine the bearing pile of pile. Design charts will be used for determining the location of neutral plane. Thickness ratio is found 0.66 and cohesion ratio is (10/50) = 0.2. Using thickness ratio and cohesion ratio, the location of neutral plane is found at 20.1 m from design chart of Fig. 4.21.

Considering reduction factor $\mathbf{R_f}$ for applied loads is 0.1, the final position of neutral plane is 18.1 m from pile head.

The Using Equation (4.2) to calculate downdrag loads, $\mathbf{Q_N}$ and shaft resistance, $\mathbf{Q_s}$.

$$\mathbf{Q_N} = 805 \text{ kN}$$

$$\mathbf{Q_s} = 1267 \text{ kN}$$

The tip resistance, $\mathbf{Q_t}$ can be calculated using the following formula

$$\mathbf{Q_t} = (\mathbf{c}\ Nc) * (\pi d^2/4)$$

An appropriate value for Nc is 9 and cohesion, **c** at the zone of pile tip is 50, therefore,

$$\mathbf{Q_t} = 88.2 \text{ kN}$$

Therefore, allowable bearing capacity of pile,

$$\mathbf{Pa} = \frac{\mathbf{Qs} + \mathbf{Q_t}}{FS} - \mathbf{Q_N}$$

$$= \frac{1267 + 88.2}{2} - 805 = -127 \text{ kN}$$

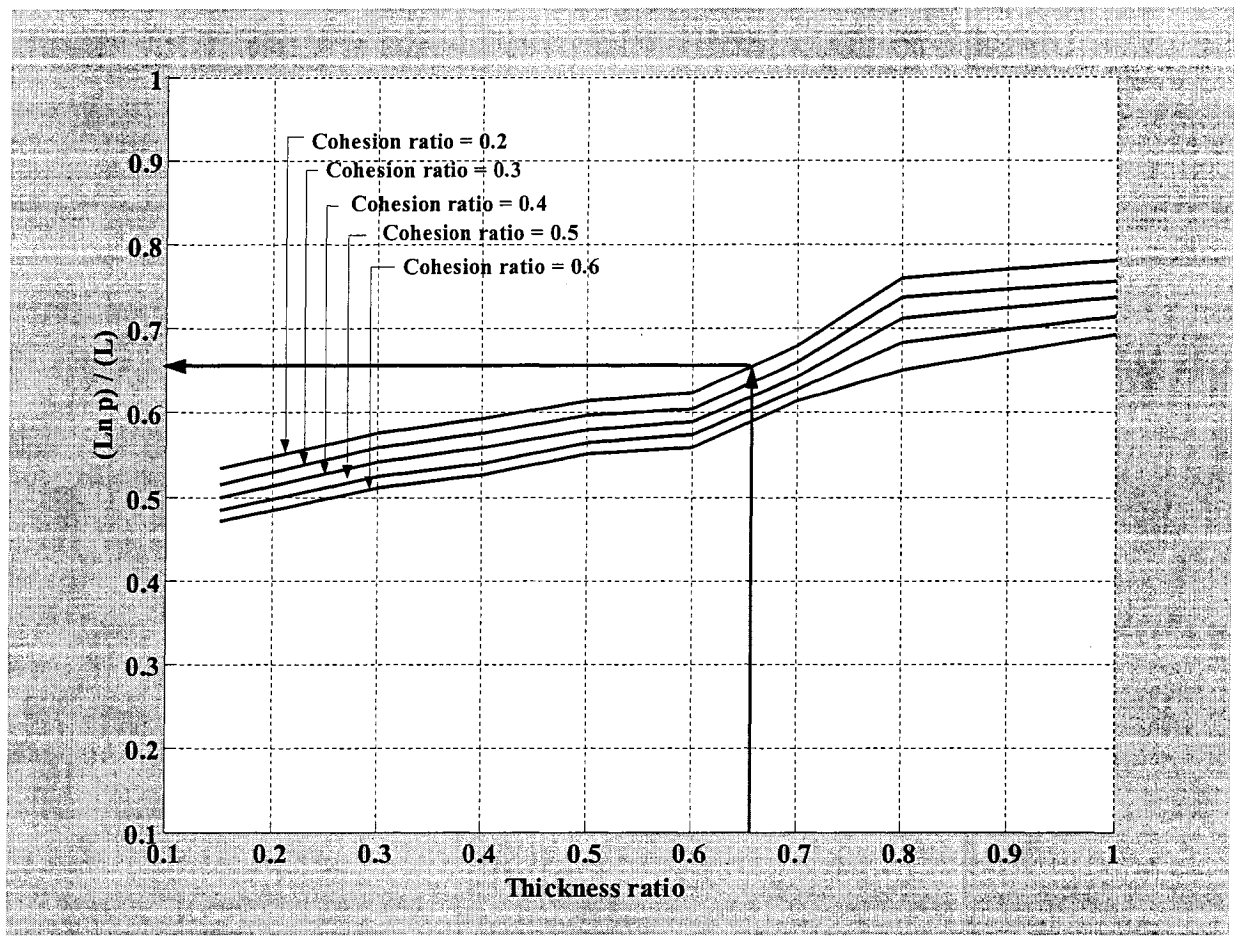

Fig. 4.24 Location of neutral plane (Surcharge loads = 50 kPa, cohesion ratio = 0.2 and thickness ratio = 0.66)

CHAPTER 5

CONCLUSION AND RECOMMENDATIONS

5.1 Conclusion

A numerical model was developed using the coupled consolidation method of analysis and the finite element technique to simulate the case of a single pile driven in clay layers and subjected to surcharge loading. Based on the results of the present investigation, the following conclusion can be drawn:

1. Coupled consolidation analysis together with the numerical model developed herein provides a powerful technique to investigate time dependency of skin friction and neutral plane location.
2. The magnitude of negative skin friction along the pile's shaft depends on the value of surcharge loads applied on the surrounding soil and the shear strength of the underlying soil layers.
3. The location of the neutral plane increases due to the decrease of cohesion ratio of the clay layers and it does not change significantly with the ratio of pile length/diameter.
4. In case of piles driven in soft clay layer overlying a medium to stiff clay of infinite depth, the neutral plane location varies approximately between one half to three fourth of the pile length during the drained period for thickness ratio varies between zero to one and for all cohesion ratios.

5. A significant drop in the location of neutral plane occurs at the end of the undrained period and it varies with time during the drained period, especially for higher thickness ratios.
6. During the drained period, the skin friction is gradually increases with time along the pile's shaft, as consolidation of soil progresses.
7. Design procedure and design charts are presented for predicting the location of neutral plane and for computing the allowable bearing capacity of single pile. This design chart will assist designers in establishing the length of bitumen coating on the pile's shaft.

5.2 Recommendations for future research

1. The development of the negative skin friction for piles in multilayered clays.
2. The variation of cohesion and elasticity of soil along the depth can be taken into account in order to calculate downdrag loads.
3. Numerical analysis can be conducted based on present model to investigate negative skin friction on battered piles.

REFERENCES

1. **Biot, M. A. (1941),** "General theory of three-dimensional consolidation," J. Applied Physics, 12, 155.
2. **Bjerrum, L. and Johannessen, I. J. (1965),** "Measurement of the compression of a steel pipe to rock due to settlement of the surrounding clay," Proc. 6th ICSMFE, Montreal, vol. 2 „pp. 261-264 .
3. **Bjerrum, L. , Johannessen, I. J. , and Eido, O.(1969),** " Reduction of skin friction on steel piles to rock," Proc. 7th ICSMFE , Mexico, vol. 2 , pp. 27-34 .
4. **Bozozuk, M. (1972),** "Downdrag measurements on a 160 ft. floating pipe test pile in marine clay," Can. Geotech. J., Vol. 9, pp.127- 136.
5. **Buisson, M., Ahu, J., and Habib, P. (1960),** " Le Frottement Negatif ," Annales de L'Institut Francis du batiment et des Travaux Publics, Sols et Foundation No. 31, pp.29 – 46.
6. **Bowels, J. E. (1997),** Foundation Analysis and Design, McGraw-Hill Companies, Inc.
7. **Chow, Y. K. , Lim, C. H. and Karunatatne, G. P. (1996),** " Numerical modeling of negative skin friction on pile groups", Computers and Geothechnics, 18(3), pp. 201-224.
8. **Craig, R. F. (1978),** Soil Mechanics, Van Nostrand Rinhold Company Ltd., England.
9. **Endo, M. Minov, A., Kawaski, T, and Shibata, T.(1969),** " Negative skin friction acting on steel pipe-piles in clay," Proc. 7th Int. Conf. SMFE, Mexico,2, pp.85-92.

10. **Fellinus, B. H. (1972),** "Downdrag on piles in clays due to negative skin friction", Can. Geotech. J. 9(4), pp. 325 – 327.

11. **Fellenius, B. H.,(1988),** " Unified Design of piles and Pile groups," Transportation Research Board, Washington, D. C., Transportation Research Record, No. 1169, pp.75 -82.

12. **Hanna, A. and Sharif, A. (2006),** "Negative skin friction on single piles in clay subjected to direct and indirect loading," In Press, Intl. Jour. of Geomechanics, ASCE.

13. **Indraratna, B., Balasubramaniam., A. S., Phamvan , P. and Wong, Y. K.(1992),** "Development of negative skin friction on driven piles in soft Bangkok clay," Can. Geotech. J., 29, pp.393 – 404.

14. **Lee, C. Y., (1993),** "Pile groups under negative skin friction," J. Geotech. Engrg., ASCE, 119(10), pp.1585-1599.

15. **Lee, C .J. and Ng, C. W. W. (2004),**" Development of downdrag on piles and pile groups in consolidating soil", J. Geotech. and Geoenvironmental Engrg. ASCE, pp.905-914.

16. **Leung, C. F., Radhakrishnan, R., and Tan, S. (1991),** "Performance of precast driven piles in marine clay, " J. Geotech. Engrg., ASCE,117(4), pp.637 – 657.

17. **Matyas, E. L. and Santamarina, J. C., (1994),** "Negative skin friction and the neutral plane," Can. Geotech. J. 31, pp.591-597.

18. **Poorooshasb, H. B. , and Bozozuk (1967),** " Skin friction on a single pile to bedrock ," Proc. 3rd Pan-American Conf. On S.M. & F.E . , Caracas, Venezuela, Vol. 1, pp.613-621.

19. **Poorooshasb, H. B., Alamgir, M., and Miura, N.(1996)** , " Negative skin friction on rigid and deformable piles, " Computer and Geotechnics, 18(2), pp.109-126.

20. **Poulos, H. G. and Davis, E. H. (1972),** "The development of negative friction with time in end-bearing piles," Aust. Geomechanics Jour., G2 (1), pp.11-20.

21. **Scientific Manual**, PLAXIS Version 8, A Two-dimensional finite element computer program.

22. **Shen, W. Y. and Teh, C. I. (2002),** "A variational solution for downdrag force analysis of pile groups", The Intl. J. of Geomechanics 2(1), pp.75 -91.

23. **Terzaghi, K. and Peck, R. B.(1948),** Mechanics in Engineering Practice, John Wiley and Sons, New York.

24. **Tomlinson, M. J. (1975),** "Foundation design and Construction," 3rd Edition, Pitman Publishing, London, England.

25. **Vesic, A. S.(1977),** "Design of pile foundations," Synthesis of Highway Practice No. 42, National Cooperative Highway Research Program, Transportation Research Board, Washington, D. C.

26. **Walker, L. K. and Darvall, P. L. P. (1973),** "Dragdown on coated and uncoated piles," Proc. 8th ICMFE, Moscow, 2.1, pp.257 -262.

27. **Wong, K. S. and Teh, C. I. (1995),** "Negative skin friction on piles in layered soil deposits," J. Geotech. Engrg. Div., ASCE, 121(6), pp.457-465.